ANNALS OF PHYSICS **144**, 282–344 (1982)

Perturbative QCD and Weak Asymmetries in Lepton Pair Production*

DAVID J. E. CALLAWAY

High Energy Physics Division, Argonne National Laboratory, Argonne, Illinois 60439,† and Department of Physics, FM-15, University of Washington, Seattle, Washington 98195

Received August 31, 1981

The interference of electromagnetic and weak production mechanisms for lepton pair production may give rise to several effects which violate parity and charge symmetry. These effects are generally of the order of 1% for dilepton masses of 10 GeV. The theoretical calculations presented here show that experimental studies of these asymmetries may be useful. In particular, measurements of these asymmetries in collisions of pions with polarized protons may lead to a greatly enhanced understanding of the polarization distribution of quarks in a polarized proton. The polarization structure of the d quark is shown to be of special interest. Measurement of the parity-violating asymmetries in proton-polarized proton collisions may prove to be a sensitive probe of the flavor symmetry of the proton antiquark sea. Analysis of the parity conserving charge asymmetry (which is predicted to occur in collisions of unpolarized hadrons) allows a unique further test of the Drell–Yan model for lepton pair production, as well as of our understanding of weak interactions.

The above asymmetries mentioned are computed within the framework of the parton model. The focus of this work is on the asymmetries calculated with the inclusion of first-order perturbative QCD effects. The asymmetries are calculated in a differential form for values of the dilepton transverse momentum large compared with the typical ($\sim$1 GeV) scale of nonperturbative effects, and also in a form in which this transverse momentum has been integrated over. Corrections to the parton model results, which can be large, show rather different structure for the various asymmetries.

A parity-violating asymmetry which may occur in collisions of *unpolarized* hadrons is also discussed. This asymmetry is very sensitive to the nonperturbative structure of hadrons, and is estimated to be approximately 0.01% for dilepton masses of 10 GeV.

INTRODUCTION

Although first observed [1] as a background effect in a search for the intermediate vector boson, the production of lepton pairs in hadronic collisions has turned out to

* This report was prepared as an account of work sponsored by the United States Government. Neither the United States nor the United States Department of Energy, nor any of their employees, nor any of their contractors, subcontractors, or their employees, makes any warranty, express or implied, or assumes any legal liability or responsability for the product or process disclosed, or represents that its use would not infringe privately-owned rights.

The U.S. Government's right to retain a nonexclusive, royalty-free license in and to any copyright covering this paper is acknowledged.

† Present address.

0003-4916/82/140282-63$05.00/0

Copyright © 1982 by Academic Press, Inc.
All rights of reproduction in any form reserved.

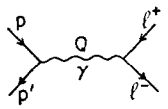

FIG. 1. The Drell-Yan mechanism of lepton pair production. A quark of momentum p from the hadron annihilates an antiquark of momentum p' from another struck hadron producting a virtual photon of momentum Q. The photon then decays to a pair of leptons of momenta l^+ and l^-.

be a major testing ground for models of the strong interaction. The (now) standard model for this process was proposed by Drell and Yan [2] after the fashion of the parton model [3]. In the Drell–Yan model a massless quark from one (beam) hadron annihilates a massless antiquark from another hadron, and produces a virtual photon of large mass $\sqrt{Q^2}$ (see Fig. 1), which then couples to a pair of leptons.

The Drell–Yan mechanism fits naturally into the framework of the parton model, wherein hadrons are constructed out of effectively noninteracting subunits called "partons." These partons are today considered to be the quarks and gluons of quantum chromodynamics [4] (QCD). With the use of asymptotic freedom [5]—the vanishing of the effective (or "running") strong coupling constant $\alpha_s(Q^2)$ in the limit of large momentum transfers—the parton model can be shown to be consistent with perturbative QCD [6–9]. In the extended perturbative QCD–parton model framework the short distance behavior of QCD is handled by treating quarks and gluons as if they were free particles on their mass shell.[1] The interactions of quarks and gluons are calculated in a perturbative expansion in $\alpha_s(Q^2)$. The resulting cross sections are then convoluted with empirically measured quark/parton distributions to give hadronic cross sections. These quark/parton distributions represent the nonperturbative long-distance behavior of the theory and cannot presently be calculated directly from QCD. Outgoing quarks and gluons are assumed to fragment into hadrons with unit probability. The details of such fragmentation are ignored in this calculation, and outgoing quarks and gluons are treated as final state particles on their mass shell.

In this perturbative formalism two types of singularities arise. One is the infrared singularity from the bremsstrahlung of soft gluons, a difficulty familiar from QED. Such singularities disappear if the gluon energy is bounded from below. Infrared singularities also cancel order by order in α_s if all elastic and inelastic scattering contributions are summed.

The other type of singularity which appears is a "collinear" or "mass" singularity, which occurs whenever a massless quark emits a collinear massless gluon [7]. These singularities can be consistently absorbed into Q^2-dependent (nonscaling) quark/parton distributions [7, 8]. The important feature of QCD is that these singularities are identical for lepton pair production and deep inelastic scattering [7–9].

[1] Corrections to this picture are of "higher twist" and terms which behave as powers of M^2/Q^2, where M has the dimensions of a mass and characterizes nonperturbative aspects of QCD.

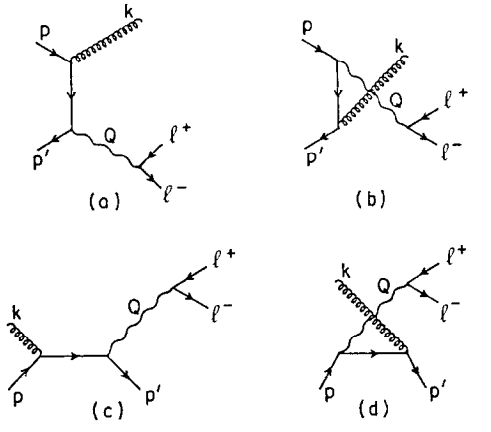

FIG. 2. Perturbative QCD corrections to the direct electromagnetic proces illustrated in Fig. 1. (a) and (b) involve annihilating quarks and antiquarks of momenta p and p', respectively, which produce a gluon of momentum k and a lepton pair with momenta l^+ and l^- through a virtual photon of momentum Q. (c) and (d) show the production of lepton pairs and a quark of momentum p' from an initial gluon of momentum k and an initial quark of momentum p. These latter two diagrams also give rise to effects of order α_s, the strong coupling constant.

The perturbative QCD corrections to the simple Drell–Yan process also contribute to the transverse momentum $|\mathbf{Q}_\perp|$ of the lepton pair. The order α_s contribution to this transverse momentum arises from the diagrams in Fig. 2. To this order, the diagrams in Fig. 3 also contribute; however, they do not add to the transverse momentum of the lepton pair.

Lepton pairs can also be produced by a weak neutral current, as shown in Figs. 4–6. These diagrams are analogous to the processes shown in Figs. 1–3 except that a virtual Z^0 replaces the virtual photon. The interference of the weak neutral current

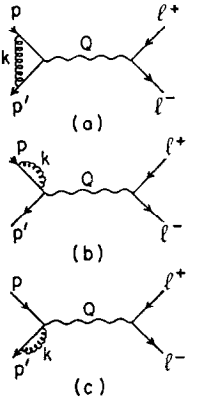

FIG. 3. Virtual gluon correction to the Drell–Yan diagram in Fig. 1. The interference of these diagrams with those of Fig. 1 produces an effect of the order of α_s, the strong coupling constant.

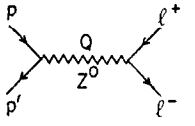

FIG. 4. The analog of the diagram Fig. 1, but with a virtual Z^0 instead of a virtual photon.

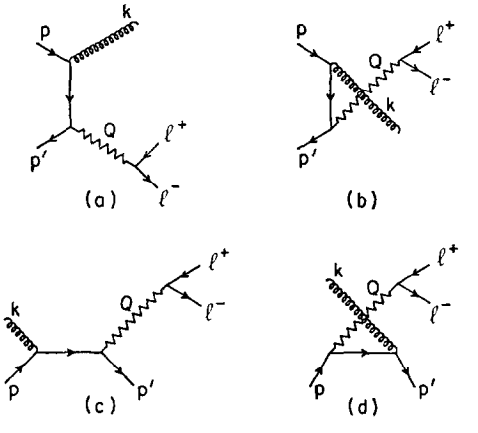

FIG. 5. The analogs of the diagrams Fig. 2, with a virtual Z^0 replacing the virtual photon.

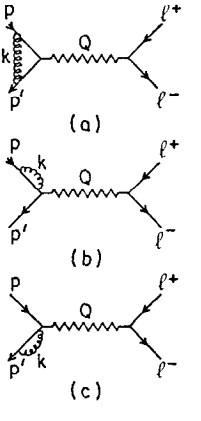

FIG. 6. The analogs of the diagrams Fig. 3, with a virtual Z^0 replacing the virtual photon.

diagrams with the electromagnetic diagrams gives rise to several parity and charge symmetry violating effects which can occur in collisions of hadrons with polarized or unpolarized hadrons. These asymmetries have been discussed previously in the context of the parton model [12–16].

Experimental study of these asymmetries can provide us with unique information on the polarization structure of the proton. In particular, given the u and d quark/parton distributions, the measurement of these asymmetries in pion-polarized proton collisions help to determine the corresponding distributions for polarized u and d quarks *separately*. The polarization distribution of the d quark is especially interesting–some novel possibilities are discussed later. It should also be kept in mind that little is known about the polarization distribution of the d quark in the proton, since experiments such as polarized ep scattering only determine a combination of the u and d quark polarization distributions. The u quark contribution in this case presumably dominates and makes extraction of the (much smaller) d quark contribution difficult.

Another interesting result arising from the parton model analysis concerns the flavor $SU(2)$ symmetry of the proton antiquark/parton ("sea") distributions. The parity-violating asymmetries may show a sign change as a function of the scaling variables in proton-polarized proton collisions if the $\bar{d}$ antiquark/parton distribution is much larger than the corresponding $\bar{u}$ distribution at large momentum fractions [13]. One example of such flavor $SU(2)$ asymmetric distributions was proposed by Field and Feynman [18].

Finally, it should be noted that the form of the weak interaction also can be studied by measuring the weak asymmetries in polarized and unpolarized hadron collisions. These asymmetries are proportional to the vector and axial vector electroweak charges of the constitutent quarks and leptons; thus the data on these asymmetries can help determine these charges.

Correction to the asymmetries as calculated in the parton model arise through the effects of perturbative QCD. The analysis of these corrections forms the major portion of this paper. The inclusion of perturbative QCD effects can also give rise [19] to a new parity-violating asymmetry (proportional to the pseudoscalar triple product of the hadron beam direction and the lepton pair momenta) which arises in *unpolarized* hadron–hadron collisions. This effect requires the inclusion of nonperturbative aspects of confinement, and is discussed here in detail.

II. Theoretical Review

The neutral weak lepton and quark currents illustrated in Fig. 4 are given by

$$j_l^\mu = \bar{l}(V_l + A_l\gamma_5)\,\gamma^\mu l, \tag{1a}$$

$$j_q^\mu = \bar{q}(V_q + A_q\gamma_5)\,\gamma^\mu q, \tag{1b}$$

respectively. In the Weinberg–Salam model [20], augmented by the GIM mechanism [21], the coupling constants are

$$V_l = \frac{-e}{4 \sin\theta_W \cos\theta_W}(1 - 4\sin^2\theta_W), \tag{2a}$$

$$A_l = \frac{-e}{4 \sin\theta_W \cos\theta_W}, \tag{2b}$$

$$V_q = \frac{e}{4 \sin\theta_W \cos\theta_W}\left(2T_3 \frac{4e_q}{e}\sin^2\theta_W\right), \tag{2c}$$

$$A_q = \frac{e}{4 \sin\theta_W \cos\theta_W}(2T_3) \tag{2d}$$

to lowest order in the weak interaction. In Eqs. (2), e is the *magnitude* of the charge on the electron, e_q is the electric charge of the quark q, T_3 is the third component of the weak isospin of the quark q ($+\frac{1}{2}$ for u quarks and $-\frac{1}{2}$ for d quarks, etc.), and θ_W is the Weinberg mixing angle. The mass of the exchanged Z^0 boson in Fig. 4 is then given in terms of the Fermi weak coupling constant G_F by

$$M_Z^2 = e^2/(4\sqrt{2}\, G_F \sin^2\theta_W \cos^2\theta_W). \tag{2e}$$

With the above definitions, it is straightforward to calculate the cross section for a quark of helicity h ($= \pm 1$) and momentum p_μ to annihilate with an unpolarized antiquark of momentum p'_μ into a lepton pair (with momenta l_μ^+, l_μ^-) via Fig. 1 (EM) and via the interference of Figs. 1 and 4 (EW). With the inclusion of a color factor of 1/3, these cross sections are [13]

$$\underset{\text{parton}}{d\sigma_h^{\text{EM}}(q\bar{q})} = \frac{1}{3}\frac{(e_q/e)^2(e_l/e)^2}{(p\cdot p')^3}\frac{1}{2}\alpha^2(p\cdot l^+ p'\cdot l^- + p\cdot l^- p'\cdot l^+)$$
$$\times \delta^{(4)}(p' + p - l^+ - l^-)\frac{d^3l^+ d^3l^-}{l_0^+ l_0^-}, \tag{3a}$$

$$\underset{\text{parton}}{d\sigma_h^{\text{EW}}(q\bar{q})} = \frac{1}{3}\frac{(e_q/e)(e_l/e)}{(p\cdot p^2)^2(2p\cdot p' - M_Z^2)}\frac{\alpha}{2\pi}\{V_l(V_q - hA_q)$$
$$\times (p\cdot l^+ p'\cdot l^- + p\cdot l^- p'\cdot l^+) + \tfrac{1}{2}A_l(A_q - hA_l)p\cdot p'$$
$$\times (p - p')\cdot(l^+ - l^-)\}\,\delta^{(4)}(p + p' - l^+ - l^-)$$
$$\times \frac{d^3l^+ d^3l^-}{l_0^+ l_0^-}, \tag{3b}$$

where e_l is the leptonic charge, $\alpha = e^2/4\pi$ is the fine-structure constant, all masses except that the Z^0 are neglected and unspecified conventions follow those of Bjorken and Drell [22]. It is convenient to define the variables

$$\begin{aligned} Q_\mu &\equiv l_\mu^+ + l_\mu^-, \\ l_\mu &\equiv l_\mu^+ - l_\mu^-, \end{aligned} \tag{4a}$$

from which follow the Jacobian identities

$$\begin{aligned} \frac{d^3l^+}{l_0^+}\frac{d^3l^-}{l_0^-} &= \frac{d^3Q}{2Q_0}\cdot\frac{Q_0}{Q_0^2 - l_0^2}\,d^3l \\ &= \frac{d^3Q}{2Q_0}\,dQ^2\,\frac{d^3l}{2l_0}\,\delta(l\cdot Q) \\ &= \frac{d^3Q}{2Q_0}\,dQ^2\left(\frac{1}{2}\frac{|l|^3}{Q - Q_0}\right)d^2\Omega_l, \end{aligned} \tag{4b}$$

where the relation $l^2 = 4m_l^2 - Q^2 \simeq -Q^2$ has been used.

For comparison with the $o(\alpha_s)$ contribution to the quark–antiquark annihilation cross section, the corresponding parton model result is expressed in terms of the propagator momenta k' and k'' defined by

$$\underset{\text{annihilation}}{q\bar{q}} \begin{cases} k' \equiv Q - p' \\ k'' \equiv p - Q. \end{cases} \tag{4c}$$

This definition holds only for $q\bar{q}$ annihilation processes. A different notation is used for processes initiated by gluons.

The electromagnetic and electroweak interference cross section Eqs. (3) can be expressed in terms of these new variables. One example is given by

$$\begin{aligned} &(p\cdot l^+)(p'\cdot l^-) + (p'\cdot l^+)(p\cdot l^-) \\ &\quad = \tfrac{1}{8}[(Q^2 - k'^2)(Q^2 - k''^2) + 4l\cdot k' l\cdot k''], \end{aligned} \tag{5}$$

where quark masses and binding effects are neglected (i.e., $p^2 = p'^2 = 0$). The energy-momentum constraint $p + p' = Q$ then gives

$$k'^2 = k''^2 = 0 \tag{6a}$$

and

$$l\cdot k' l\cdot k'' = \tfrac{1}{2}[(l\cdot k')^2 + (l\cdot k'')^2]. \tag{6b}$$

The electromagnetic and electroweak interference contributions to the quark–antiquark annihilation cross section become

$$d\sigma_{h\ \text{parton}}^{\text{EM}}(q\bar{q}) = \frac{1}{3}\frac{(e_q/e)^2(e_l/e)^2}{(Q^2)^3}\frac{1}{8}\alpha^2[(Q^2)^2 + 2(l\cdot k')^2 + 2(l\cdot k'')^2] \times \delta^{(4)}(k''-k'+Q)\frac{d^3Q d^3l}{Q_0^2 - l_0^2}, \tag{7a}$$

$$d\sigma_h^{\text{EW}}(q\bar{q}) = \frac{1}{3}\frac{e_q}{e}\frac{e_l}{e}\frac{1}{(Q^2)^2(Q^2-M_z^2)}\frac{1}{8\pi}\{V_l)V_q - hA_q) \times [(Q^2)^2 + 2(l\cdot k')^2 + 2(l\cdot k'')^2] + 2A_l(Aq - hVq)\,Q^2 l(k'+k'')\}\,\delta^{(4)}(k''-k'+Q)\frac{d^3Q d^3l}{Q_0^2-l_0^2}. \tag{7b}$$

The cross section for a hadronic collision is calculated by convoluting the quark cross section Eqs. (7) with the approproate quark/parton distributions. For example, the cross section for lepton pair production from $\pi^- p$ collisions is given schematically in terms of the $u\bar{u}$ quark annihilation cross section $d\sigma_{u\bar{u}}$ by

$$d\sigma_{\pi^- p} = \iiiint dx_1\, d^2p_2\, dx_2\, d^2p_2' dN_u\, dN_{\bar{u}}^{\pi}\, d\sigma_{u\bar{u}} \tag{8a}$$

The generic quark and antiquark distributions $dN_{\bar{q}}$ and $dN_{\bar{q}}$ are given by

$$\begin{aligned} dN_q^p &= \delta^2(\mathbf{p}_\perp)\, q_p(x_1, Q^2), \\ dN_{\bar{q}}^{\pi} &= \delta^2(\mathbf{P}'_\perp)\, \bar{q}_\pi(x_2, Q_2) \end{aligned} \tag{8b}$$

in the naive parton model. Here, $q_p(x_1, Q^2)$ is the (scale-dependent) renormalized distribution in longitudinal momentum fraction x_1 of quarks of flavor q (e.g., u, d, s) in a proton. The analogous distribution for $\bar{q}$ quarks in a pion is denoted by $\bar{q}_\pi(x, Q^2)$.

For the calculations presented in Section III, the naive parton distributions Eq. (8b) suffice, as the effects considered are not sensitive to the small initial transverse momentum of the quark or gluon. However in Section IV an effect is calculated which is sensitive to such nonperturbative effects. The transverse momentum distributions of the initial quarks and antiquarks are parametrized as

$$\begin{aligned} dN_q^p &= \frac{1}{\sigma^2} e^{-\mathbf{p}_\perp^2/\sigma^2} q_p(x_1, Q^2), \\ dN_{\bar{q}}^{\pi} &= \frac{1}{\sigma^2} e^{-\mathbf{p}'^2/\sigma^2} \bar{q}_\pi(x_2, Q^2) \end{aligned} \tag{8c}$$

with $\sigma \simeq 0.5$ GeV. Such distributions are used [19] to describe *effectively* the internal transverse momentum of quarks (and gluons) within hadrons. The "smeared" distributions Eq. (8c) reduce to the naive parton model distributions of Eq. (8b) in the limit $\sigma \to 0$.

In the frame where the incoming quarks are collinear in the $\hat{z}$ direction, the hadron containing the antiquark (e.g., the pion) has momentum $P_0\hat{z}$, while the hadron containing the quark (e.g., the proton) has momentum $-P_0\hat{z}$ ($P_0 \simeq \frac{1}{2}\sqrt{s}$). The quarks then have momenta (ignoring the transverse momentum of the quark inside the hadron)

$$\mathbf{p} = -x_1 p_0 \hat{z}, \qquad \mathbf{p}' = x_2 p_0 \hat{z}, \tag{9}$$

while four-momentum conservation requires

$$Q^2 = x_1 x_2 s, \qquad Q_3 = (x_1 - x_2) P_2 \equiv x_F P_0. \tag{10}$$

The following variables are now defined:

$$\cos\theta_l \equiv \boldsymbol{l} \cdot \hat{z}/|\boldsymbol{l}|, \tag{11a}$$

$$\tau \equiv Q^2/s. \tag{11b}$$

Then with use of the relations $l \cdot Q = 0$ and $l^2 \cong -Q^2$ it follows that

$$l \cdot k'' = l \cdot k'' = \frac{-l^2}{2} \frac{\cos\theta_l}{\sqrt{1 + (x_F^2/4\tau)\sin^2\theta_l}} \equiv \frac{1}{2}(-l^2)\cos\chi. \tag{12}$$

Note that the relations Eq. (12) only hold for the parton model calculation.

The electromagnetic and electroweak contributions to the quark cross section (Eqs. (7)) in the context of the parton model can then be written

$$d\sigma_{h\,\text{parton}}^{\text{EM}}(q\bar{q}) = \frac{1}{3}\left(\frac{e_q}{e}\right)^2 \left(\frac{e_l}{e}\right)^2 \frac{\alpha^2}{Q^2} \tfrac{1}{2}(1 + \cos^2\chi)\,\delta^2(Q_\perp)\,\delta(x_1 - \bar{x}_1)\,\delta(x_2 - \bar{x}_2) \times \frac{1}{s}\frac{d^3Q\,d^3l}{Q_0^2 - l_0^2}, \tag{13a}$$

$$d\sigma_{h\,\text{parton}}^{\text{EW}}(q\bar{q}) = \frac{1}{3}\frac{e_q}{e}\frac{e_l}{e}\frac{1}{Q^2 - M_Z^2}\frac{\alpha}{2\pi}\{V_l(V_q - hA_q)(1 + \cos^2\chi) + 2A_l(A_q - hV_q)\cos\chi\} \times \delta^2(\mathbf{Q}_\perp)\,\delta(x_1 - \bar{x}_1)\,\delta(x_2 - \bar{x}_2)\frac{1}{s}\frac{d^3Q\,d^3l}{Q_0^2 - l_0^2}, \tag{13b}$$

where

$$\bar{x}_1 = \tfrac{1}{2}(\sqrt{4\tau + x_F^2} - x_F), \tag{14a}$$

$$\bar{x}_2 \equiv \tfrac{1}{2}(4\sqrt{4\tau + x_F^2} + x_F). \tag{14b}$$

The familiar results for the lepton c.m. frame (such as in e^+e^- annihilation) appear for $x_F = 0$, where $\cos\chi = \cos\theta_l$. The term in Eq. (13b) proportional to $V_l V_q$ is essentially an order Q^2/M_Z^2 correction to the electromagnetic cross section Eq. (13a) and can be ignored, as only $Q^2 \ll M_Z^2$ is presently possible experimentally. Since the term in Eq. (13b) proportional to $hV_l A_q$ is odd in the quark helicity, it violates parity [12–15]. This term gives rise to an effect called [13] the "helicity asymmetry." The terms proportional to A_l are asymmetric in the lepton momenta (as $\cos\chi$ changes sign under the interchange $l_\mu^+ \leftrightarrow l_\mu^-$) and give rise to two effects [12–16]: a parity-violating "charge-helicity asymmetry" proportional to $hA_l V_q$ and a parity-conserving "charge asymmetry" proportional to $A_l A_q$. In the parton model without perturbative QCD corrections the existence of a parity-violating effect requires a nonzero average quark polarization, and thus at least one polarized initial hadron.

The helicity asymmetry, a_h is defined for hadron–polarized hadron collisions by

$$a_h(l^+, l^-) = a_h(l^-, l^+) \equiv \left(\frac{d^6\sigma_+(l^+, l^-)}{d^3l^+\, d^3l^-} - \frac{d^6\sigma_-(l^+, l^-)}{d^3l^+\, d^3l^-} + [l^+ \leftrightarrow l^-]\right) \times \left(\frac{d^6\sigma_+(l^+, l^-)}{d^3l^+\, d^3l^-} + \frac{d^6\sigma_-(l^+, l^-)}{d^3l^+\, d^3l^-} + [l^+ \leftrightarrow l^-]\right)^{-1} \tag{15}$$

where $d\sigma_\pm$ refers to the helicity of the polarized hadron. Similarly, the charge-helicity asymmtery a_{ch} is defined by

$$a_{\text{ch}}(l^+, l^-) = -a_{\text{ch}}(l^-, l^+) \equiv \left(\frac{d^6\sigma_+(l^+, l^-)}{d^3l^+\, d^3l^-} - \frac{d^6\sigma_-(l^+, l^-)}{d^3l^+\, d^3l^-} - [l^+ \leftrightarrow l^-]\right) \times \left(\frac{d^6\sigma_+(l^+, l^-)}{d^3l^+\, d^3l^-} + \frac{d^6\sigma_-(l^+, l^-)}{d^3l^+ d^3l^-} + [l^+ \leftrightarrow l^-]\right)^{-1} \tag{16}$$

The charge asymmetry is defined for polarized or unpolarized hadron–hadron collisions by

$$a_c(l^+, l^-) = -a(l^-, l^+) \equiv \left(\frac{d^6\sigma(l^+, l^-)}{d^3l^+\, d^3l^-} - [l^+ \leftrightarrow l^-]\right) \times \left(\frac{d^6\sigma(l^+, l^-)}{d^3l^+\, d^3l^-} + [l^+ \leftrightarrow l^-]\right)^{-1}. \tag{17a}$$

With Eqs. (8)–(13), the charge asymmetry can be calculated in the context of the parton model in the absence of polarized quarks. For *π-unpolarized p* collisions it is given by [13]

$$\left.\begin{matrix} a_c^{\pi^+ P}(l^+, l^-) \\ a_c^{\pi^- p}(l^+, l^-) \end{matrix}\right\} = \left\{\begin{matrix} \dfrac{A_u}{(e_u/e)} \\ \dfrac{A_d}{(e_d/e)} \end{matrix}\right\} \frac{A_l}{e_l/e} \frac{1}{2\pi\alpha} \left(\frac{Q^2}{Q^2 - M_Z^2}\right) \frac{2\cos\chi}{1+\cos^2\chi} \tag{17b}$$

where it has been assumed that valence quark annihilation is the dominant process.

In order to relate the parity-violating asymmetries for hadrons (a_h, a_{ch}) to quark cross sections, the distribution functions describing polarized quarks within a polarized hadron are required. The parity-violating contributions to the cross section are calculated in the fashion of Eqs. (8), with the (generic) quark distribution $q(x, Q^2)$ replaced by

$$\Delta q(x, Q^2) \equiv q^+(x, Q^2) - q^-(x, Q^2), \tag{18}$$

where $q^+(x, Q^2)$ $[q^-(x, Q^2)]$ is the distribution in longitudinal momentum fraction of quarks of flavor q with positive [negative] helicity in a proton of positive helicity.

Calculations [23] based on perturbative QCD indicate that in some kinematic regions a significant amount of sea quark polarization may occur. The sea distributions are negligible however for large momentum fractions where the effects of interest occur. Furthermore, the effects of sea polarization are generally small. Sea polarization is therefore neglected in this paper.

For u and d quarks in a proton, functions $\bar{\alpha}(x, Q^2)$ and $\bar{\beta}(x, Q^2)$ are defined by (13),

$$\begin{aligned} \bar{\alpha}(x, Q^2)\, u(x, Q^2) &= \bar{\alpha}(x, Q^2)[u^+(x, Q^2) + u^-(x, Q^2)] \\ &\equiv u^+(x, Q^2) - u^-(x, Q^2) \\ &\equiv \Delta u(x, Q^2), \end{aligned} \tag{19a}$$

$$\begin{aligned} \bar{\beta}(x, Q^2)\, d(x, Q^2) &= \bar{\beta}(x, Q^2)[d^+(x, Q^2) + d^-(x, Q^2)] \\ &\equiv d^+(x, Q^2) - d^-(x, Q^2) \\ &\equiv \Delta d(x, Q^2). \end{aligned} \tag{19b}$$

Since the focus of this paper is not on scaling violations (which are presumably small effects at the relevant energies) the Q^2 dependence of $\bar{\alpha}(x, Q^2)$ and $\bar{\beta}(x, Q^2)$ is suppressed in the forthcoming dicussion.

If lepton pair production in π^--polarized proton (π^+-polarized proton) collisions is assumed to take place entirely by $u\bar{u}$ $[d\bar{d}]$ annihilation, it follows from the previous discussion that the helicity asymmetry in the parton model is given by

$$\left.\begin{matrix} a_h^{\pi^- p}(l^+, l^-) \\ a_h^{\pi^+ p}(l^+, l^-) \end{matrix}\right\} = \left\{\begin{matrix} \dfrac{A_u}{(e_u/e)} \\ \dfrac{A_d}{(e_d/e)} \end{matrix}\right\} \frac{V_l}{(e_l/e)} \frac{1}{2\pi\alpha} \left(\frac{-Q^2}{Q^2 - M_Z^2}\right) \left\{\begin{matrix} \bar{\alpha}(\bar{x}_1) \\ \bar{\beta}(\bar{x}_1) \end{matrix}\right\} \tag{20}$$

which is independent of angle. In Eq. (20), the integrations over the quark and antiquark longitudinal momentum fractions x_1 and x_2 are performed with the delta functions in Eqs. (13).

The charge-helicity asymmetry a_{ch} for π-polarized p collisions is likewise given by [13]

$$\left.\begin{matrix} a_{ch}^{\pi^- p}(l^+, l^-) \\ a_{ch}^{\pi^+ p}(l^+, l^-) \end{matrix}\right\} = \left\{\begin{matrix} \dfrac{V_u}{(e_u/e)} \\ \dfrac{V_d}{(e_d/e)} \end{matrix}\right\} \frac{A^l}{(e_l/e)} \frac{1}{2\pi\alpha} \left(\frac{-Q^2}{Q^2 - M_Z^2}\right) \left(\frac{2\cos\chi}{1+\cos^2\chi}\right) \left\{\begin{matrix} \bar{\alpha}(\bar{x}_1) \\ \bar{\beta}(\bar{x}_1) \end{matrix}\right\}. \tag{21}$$

Measurement of the asymmetries Eqs. (20) and (21) in π-polarized p collisions therefore allows direct observation of the functions $\bar{\alpha}(x)$ and $\bar{\beta}(x)$. In particular, arguments discussed in detail elsewhere [13] indicate that $\bar{\beta}(x)$ may change sign as a function of x. These arguments imply a sign change in both $a_h^{\pi+p}$ and $a_{ch}^{\pi+p}$ as a function of—τ a rather dramatic experimental signature.

These arguments are based on the parton model sum rules [13]

$$\int_0^1 \bar{\alpha}(x)\, u(x)\, dx = s_3 + \tfrac{1}{2} G_A/G_V \tag{22a}$$

$$\int_0^1 \bar{\beta}(x)\, d(x)\, dx = s_3 - \tfrac{1}{2} G_A/G_V \tag{22b}$$

where s_3 is the expectation value of the contrbution of the quark spins to the total proton spin, and G_A/G_V is the ratio of the axial vector to vector coupling constants measured in neutron beta decay. If the proton spin arises entirely from quark spins rather than from orbital angular momentum or from gluons, then $s_3 = 1/2$. An $SU(3)$ argument [24] gives $s_3 \simeq 0.3$, while experimentally [25] $G_A/G_V \equiv 1.254 \pm 0.007$.

Equations (19) imply the bounds $|\bar{\alpha}(x)| \leqslant 1$, $|\bar{\beta}(x)| \leqslant 1$. Together with Eqs. (22) this implies $\bar{\beta}(x) < 0$ for some range of x. Yet calculations based on perturbative QCD [26] suggest that as $x \to 1$, the helicity of a quark approaches that of the polarized parent hadron. Then $\bar{\beta}(x) \to 1$ as $x \to 1$, implying a sign change at some value of x.

Consider proton–proton collisions. The cross section in Eq. (8a) involves a *sum* over various quark types. In the framework of the parton model, lepton pair production arises from the annihilation of a valence quark from one proton with a sea antiquark from the other incident proton. Sea quarks and gluons are assumed to be unpolarized. Contributions to the parity-violating portion of the cross section thus come from $u\bar{u}$ and $d\bar{d}$ annihilation processes only. A question that can be probed by measuring the parity-violating asymmetries is whether the $\bar{u}$ and $\bar{d}$ sea distributions are equal, i.e., if the sea is flavor $SU(2)$ symmetric. While the product of the electric and weak charges is of the same sign for $u\bar{u}$ and $d\bar{d}$ annihilation, $\bar{\alpha}(x)$ is generally greater than zero (by Eq. (22a)) by $\bar{\beta}(x)$ is generally less than zero (by Eq. (22b)).

Thus the parity-violating asymmetries a_h and a_{ch} in proton–polarized proton collisions consist of the sum of positive $u\bar{u}$ annihilation contributions and negative $d\bar{d}$ annihilation contributions and negative $d\bar{d}$ annihilation contributions. It has been suggested [18] that as $x \to 1$, $\bar{u}(x)/\bar{d}(x) \to 0$, which implies that as $x \to 1$ the dominant contribution to the parity-violating asymmetries comes from $d\bar{d}$ annihilation. Conversely for $x < 0.5$ the $u\bar{u}$ annihilation process is dominant, as there are more u quarks than d quarks and $\bar{a}(x)$ is generally larger in magnitude than $\bar{\beta}(x)$. In passing from one region of x to another, the asymmetry may change sign if the proton sea is $SU(2)$ asymmetric in this fashion [13]. If the sea is $SU(2)$ symmetric, or if $\bar{d}(x) \leqslant \bar{u}(x)$ as $x \to 1$, no such sign change occurs.

III. Perturbative QCD Effects on Weak Asymmetries

A. *Prolegomena*

Corrections to the parton model picture presented in the previous section are now calculated in a perturbation expansion in the strong coupling constant α_s ($\alpha_s = g_s^2/4\pi$ where g_s is the quark–gluon coupling). To first order in α_s these corrections appear in two different ways. First the structure functions (as measured in, e.g., deep inelastic scattering) are renormalized to order α_s and to all orders in leading logarithmic accuracy. The cross section for lepton production also has perturbative corrections of order α_s. The diagrams of Figs. 2 and 3 illustrate contributions to the parity-conserving direct electromagnetic process displayed in Fig. 1, while the corresponding diagrams for the parity-violating neutral current process of Fig. 4 are displayed in Figs. 5 and 6.

The diagrams of Figs. 2 to 6 are of two types—classified as to whether they involve real final or initial gluons (Figs. 2 and 5) or virtual gluons (Figs. 3 and 6). The lepton pair in the real gluon graphs can have a transverse momentum $\mathbf{Q}_\perp$, while the lepton pair in the virtual gluon graphs has $\mathbf{Q}_\perp = 0$ provided the initial quarks have no transverse momenta within their parent hadrons.

As mentioned in Section I, in perturbative QCD with massless quarks the graphs Figs. 2–6 are divergent. Two types of singularity occur [8–11]. The first type is the infrared singularity, which cancels among the diagrams for a particular process—the infrared singularities in Figs. 2a and 2b cancel with those from Figs. 3. The second type of singularity— the "collinear" singularity—can be absorbed into the nonscaling renormalized parton distributions. The important feature is that these singularities (and hence the nonscaling parton distributions) are the same for all processes.

The contribution to the differential lepton pair production cross section $(d^2\sigma/dQ_\perp^2)$ from the real final gluon graphs (Figs. 2a and b and 5a and b) diverge like $d(\ln^2 \delta)/d\delta$ as $\delta = |\mathbf{Q}_\perp|^2/Q^2 \to 0$. One power of the logarithm originates from the infrared singularity, the other from the collinear singularity at $\delta = 0$. The contributions of the virtual gluon graphs (Figs. 3 and 6) to this differential cross section are proportional to $\delta^2\,|\mathbf{Q}_\perp)|$, another singular function, in the limit of no

initial quark transverse momentum. When integrated over $\mathbf{Q}_\perp$, the contributions to the cross section from the real gluon graphs diverge as $\ln^2(Q^2/M^2)$ as $(Q^2/M^2) \to \infty$, where M^2 is the infrared cutoff. The corresponding with the same cutoff also have a $\ln^2(Q^2/M^2)$ term of equal magnitude but opposite sign to cancel this singularity when all contributions are summed up. Remaining terms of order $\ln(Q^2/M^2)$ from the collinear singularities are absorbed into the parton distributions [6–11]. This method for disposing of the collinear singularities is explored in detail later.

The previous discussion suggests two quantities which can be calculated in perturbative QCD. The first is the cross section for producing a lepton pair with transverse momentum large compared to the scale of nonperturbative confinement effects (i.e., $|\mathbf{Q}_\perp| \gg 0.5$ GeV). In this kinematic region the effects of the initial quark (or gluon) transverse momentum are negligible. Contributions to this cross section are necessarily of order α_s or higher in order to generate a nonzero $|\mathbf{Q}_\perp|$.

It should be noted that in order for perturbation theory to be valid, $|\mathbf{Q}_\perp|$ cannot be too small. Specifically $-\alpha_s \ln(|\mathbf{Q}_\perp|^2/Q^2) \ll 1$ must hold in order that diagrams which are higher order in α_s [and contain terms with correspondingly more powers of $\ln(|\mathbf{Q}_\perp|^2/Q^2)$] do not dominate the diagrams of lower order.

The second quantity which can be calculated is the cross section integrated over $\mathbf{Q}_\perp$, which includes terms of order (α_s) and higher. The ratios of the (differential) large $|\mathbf{Q}_\perp|$ or integrated electroweak interference cross sections to the analogous total (i.e., electromagnetic and weak) cross section are presented here to lowest order in the weak interaction.

B. *Weak Asymmetries at Large* $|\mathbf{Q}_\perp|$

1. *Quark–antiquark annihilation diagrams*

(a) ELECTROMAGNETIC CROSS SECTION. The QCD currents are defined by analogy with Eq. (1) as

$$j_i^\mu = g_s \bar{q} \left(\frac{\lambda_i}{2}\right) \gamma^\mu q, \tag{23}$$

where the λ_i are the matrices of the $SU(3)$ color group. The squared matrix element for the real final gluon process of Figs. 2a and 2b is then given by

$$|M_{\text{EM}}|^2_{\substack{q\bar{q} \\ \text{real gluon}}} = g_s^2 e_l^2 e_q^2 S_0(k', k'', Q, l), \tag{24a}$$

where

$$S_0(k', k'', Q, l) = \frac{8Q^2}{k'^2 k''^2} \{(Q^2 - k'^2)^2 + (Q^2 - k''^2)^2 + 4[(l \cdot k')^2 + (l \cdot k'')^2]\}. \tag{24b}$$

Simplifications result from using the propagator variables k' and k'' defined in Eqs. (4c). The squares of these variables are related to the usual Mandelstam variables by

$$\left\{\begin{matrix} q\bar{q} \\ \text{annihilation} \end{matrix}\right\} \qquad \begin{aligned} s' &= Q^2 - k'^2 - k''^2, \qquad & t' &= k'^2 = (Q - p')^2, \\ &= (p + p')^2, & u &= k''^2 = (p - Q)^2 \end{aligned} \tag{24c}$$

with primes denoting quark variables, as opposed to hadron variables.

The real gluon contribution to the cross section for this process is given by

$$\begin{aligned} d\sigma_{\substack{h \\ \text{real gluon}}}^{\text{EM}}(q\bar{q}) = \frac{1}{4\pi}\left(\frac{4}{9}\frac{\alpha_s}{2\pi}\right)\left(\frac{e_l}{e}\right)^2\left(\frac{e_q}{e}\right)^2 \frac{\alpha^2}{(Q^2)^2 s} S_0(k', k'', Q, l) \\ \times \delta[(k'' - k' + Q)^2]\frac{d^3Q d^3l}{Q_0^2 - l_0^2}, \end{aligned} \tag{25a}$$

where $k'' - k' + Q = k$, the four-momentum of the final gluon, and the color factor of $4/9$ is given in terms of the λ matrices by

$$\frac{1}{3}\sum_i \text{Tr}\left(\frac{\lambda^i}{2}\frac{\lambda^i}{2}\right) = \frac{4}{9} \tag{25b}$$

The parton model is introduced into Eqs. (23)–(25) by defining the quark and anti-quark four-momenta p and p' in terms of the longitudinal momentum fractions x_1 and x_2 in the hadron c.m. frame,

$$p = x_1 P_1, \qquad p' = x_2 P_2, \tag{26a}$$

$$\mathbf{P}_1 = -\hat{z}P_0, \qquad \mathbf{P}_2 = +\hat{z}P_0, \tag{26b}$$

$$s = (P_1 + P_2)^2 = 4P_0^2, \tag{26c}$$

where P_1 and P_2 are the four-momenta of the incoming hadrons which are on mass shall and are approximated as being massless ($P_1^2 = P_2^2 = 0$). It is also convenient to define the hadronic variables

$$\begin{aligned} \tilde{x}^i \equiv \frac{Q^2}{2Q \cdot P_i}, \qquad y_i \equiv \frac{x_i}{\tilde{x}_i}, \qquad i = 1, 2, \\ \delta \equiv \frac{Q^2 - \tilde{x}_1\tilde{x}_2 s}{\tilde{x}_1\tilde{x}_2 s}, \end{aligned} \tag{27a}$$

and therefore

$$\delta = \frac{|\mathbf{Q}_\perp|^2}{Q^2} \tag{27b}$$

in hadron c.m. frame. The condition that the final gluon be massless, $k^2 = 0$, then gives a relation between y_2 and y_1:

$$y_2 = y_2' \equiv \frac{(y_1 - 1)(1 + \delta)}{y_1 - (1 + \delta)}. \tag{28a}$$

The corresponding delta function is used to perform the y_2 integration in the cross section. Momentum conservation requires both y_1 and y_2 to be $\leqslant 1$, leading to the bounds

$$y_{1,\min} \equiv \frac{(1-x_2)(1+\delta)}{1-(1+\delta)\tilde{x}_2} \leqslant y_1 \leqslant \frac{1}{\tilde{x}_1} \equiv y_{1,\max} \tag{28b}$$

and similarly for y_2. Relations (28) are displayed graphically in Fig. 7. The cross section for lepton pair production from hadron–polarized hadron collisions at large $|\mathbf{Q}_\perp|$ via $\bar{q}$-polarized q electromagnetic annihilation is then

$$\begin{aligned} \underset{\text{large}|\mathbf{Q}_\perp|}{d\sigma^{\mathrm{EM}}(q\bar{q})} = & \left(\frac{4}{9}\frac{\alpha_s}{2\pi}\right)\left(\frac{e_q}{e}\right)^2\left(\frac{e_l}{e}\right)^2 \frac{1}{2\pi}\frac{\alpha^2}{(Q^2)^3}\frac{d^3l\,d^3Q}{Q_0^2-l_0^2}\,\delta(y_2-y_2') \\ & \times\left|(1+\zeta_1^2)F_1(y_1,\delta)+(1+\zeta_2^2)F_2(y_1,\delta)\right| \\ & \times q(x_1)\,\bar{q}(x_2)\,dx_2\,dx_2 \end{aligned} \tag{29a}$$

with

$$\begin{aligned} F_1(y_1,\delta) &\equiv \frac{1+\delta}{\delta}\left[\frac{1}{y_1-1}-\frac{\delta}{(y_1-1)^2}\right], \\ F_2(y_1,\delta) &\equiv \frac{1+\delta}{\delta}\left[\frac{1}{y_1-(1+\delta)}-\frac{1}{y_1}-\frac{1+\delta}{y_1^2}\right] \\ &= F_1(y_2',\delta) \end{aligned} \tag{29b}$$

and

$$\zeta_n \equiv 2\frac{\tilde{x}_n\widetilde{l\cdot P_n}}{2}; \qquad n=1,2 \tag{29c}$$

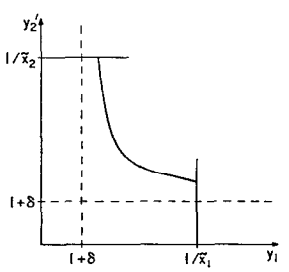

FIG. 7. Plot of y_2' versus y_1 as given by Eqs. (28). The variable y_1 ranges from $y_{1,\min}=(1-\tilde{x}_2)(1+\delta)/(1+(1+\delta)\tilde{x}_2)$ to $y_{1,\max}=1/\tilde{x}_1$.

where

$$\left.\begin{matrix}\widetilde{l\cdot P_1}\\ \widetilde{l\cdot P_2}\end{matrix}\right\} \equiv \frac{1}{2}\sqrt{s}\,\frac{|\mathbf{Q}_\perp|\cos\theta_l Q \pm Q_0\cos\theta_l}{\sqrt{Q_0^2|\mathbf{Q}|^2\cos^2\theta_{lQ}}} \tag{30a}$$

$$\to \pm\frac{1}{2}(-l^2)\cos\chi = \pm\frac{1}{2}(Q^2-4m_l^2)\cos\chi \qquad \text{as } \delta\to 0 \tag{30a}$$

with

$$\begin{aligned}|\mathbf{Q}|\cos\theta_{lQ} &\equiv \mathbf{Q}\cdot\boldsymbol{l}/|\boldsymbol{l}|\\ &= Q_3\cos\theta_e|\mathbf{Q}_\perp|\sin\theta_e\cos\phi_l\\ &= \frac{1}{2}x_F\sqrt{s}\cos\theta_l + \sqrt{Q^2\delta}\sin\theta_l\cos\phi_l\end{aligned} \tag{30b}$$

and ϕ_l defined to be the angle between $\boldsymbol{l}$ and $\mathbf{Q}$ in the plane normal to the beam direction.

The origin of the $d(\ln^2\delta)/d\delta$ divergence discussed earlier follows easily from the preceding discussion. Consider the terms in the cross section Eq. (25) proportional to

$$\iint dy_1\,dy_2\,\frac{(Q^2)^3}{k'^2k''^2}\,\delta(k^2)$$

$$= \iint \frac{Q^2\delta(k^2)}{(y_1-1)(y_2-1)}\,dy_1\,dy_2 \tag{31a}$$

$$= \iint \frac{\delta\left[y_2-(y_1-1)(1+\delta)/(y_1-(1+\delta))\right]}{y_1(y_1-1)}\,dy_1\,dy_2 \tag{31b}$$

$$\simeq \frac{1}{\delta}\int_{y_1,\min}^{y_1,\max}\frac{dy_1}{y_1-1} \qquad \text{as} \quad \delta\to 0, \tag{31c}$$

$$\simeq \frac{\ln\delta}{\delta}+\cdots \qquad \text{as} \quad \delta\to 0 \tag{31d}$$

$$= \frac{1}{2}\frac{d(\ln^2\delta)}{d\delta}+\cdots. \tag{31e}$$

If this is integrated over $|\mathbf{Q}_\perp|$ it gives rise to the $\ln^2 Q^2$ divergence discussed previously. This divergence occurs in the region of integration where the gluon is both collinear ($\delta \ll 1$) and soft ($y_1, y_2 \simeq 1$).

b. Electroweak Cross Section. The contributions of the real final gluon graphs to the electroweak interference term are of two types. The first variety (referred to as $S_0(k', k'', Q, l)$ in Eq. (24b)) is symmetric under the interchange of the lepton momenta ($l_\mu^+ \leftrightarrow l_\mu^-$, or $l_\mu \to -l_\mu$). This contribution is proportional to the squared electromagnetic matrix element, Eq. (24a). The simple proportionality of the

charge-symmetric electroweak interference term proportional to V_l and the squared electromagnetic matrix element also occurs in the parton model result Eq. (3).

The second contribution is *antisymmetric* under the interchange of the lepton momenta and is referred to as $A_0(k', k'', Q, l)$. Thus, the electroweak interference contribution to the squared matrix element is given by

$$2\,\mathrm{Re}[\bar{M}_{\mathrm{EM}} M_{\mathrm{weak}}]_{\substack{\text{real}\\ \text{gluon}}} q\bar{q} = g_s^2 e_q e_l [V_l(V_q - hA_q)\, S_0(k', k'', Q, l) + A_l(A_q - hV_q)\, A_0(k', k'', Q, l)], \tag{32a}$$

where

$$A_0(k', k'', Q, l) \equiv 32Q^2 \left[\frac{l\cdot k'}{k''^2} + \frac{l\cdot k''}{k'^2} - \frac{Q^2 l\cdot(k'+k'')}{k'^2 k''^2}\right]. \tag{32b}$$

Recall the parton model result for the electroweak interference cross section, Eqs. (7b) and (13b). In that case, there are four separate parts to the electroweak interference cross section, two of which violate parity. As discussed previously, such parity-violating effects are proportional to the quark helicity, and thus in the QCD augmented parton model their cross section involves the function $\Delta q(x_1)$ rather than $q(x_1)$. The q-polarized q electroweak interference contribution to the hadron–polarized hadron cross section at large $|\mathbf{Q}_\perp|$ is thus given by

$$\begin{aligned} d\sigma^{\mathrm{EW}}_{\substack{\text{large}\\ |\mathbf{Q}_\perp|}}(q\bar{q}) = {} & \left(\frac{4}{9}\frac{\alpha_s}{2\pi}\right)\left(\frac{e_q}{e}\right)\left(\frac{e_l}{e}\right)\frac{1}{2\pi^2}\frac{\alpha}{(Q^2)^2(Q^2-M_Z^2)}\frac{d^3l\, d^3Q}{Q_0^2 - l_0^2} \\ & \times \delta(y_2 - y_2')\, \bar{q}(x_2)\, dx_1\, dx_2 \\ & \times \{V_l[V_q q(x_1) - A_q \Delta q(x_1)]\,[(1+\zeta_1^2)\, F_1(y_1, \delta) + (1+\zeta_2^2)\, F_2(y_2, \delta)] \\ & + 2A_l[A_q q(x_1) - V_q \Delta_q(x_1)]\,[\zeta_1 F_1(y_1, \delta) - \zeta_2 F_2(y_1, \delta)]\}, \end{aligned} \tag{33}$$

where antiquark polarization is neglected as discussed previously. To calculate the cross section for, e.g., π^--polarized p collisions, the function $\Delta q(x)$ is replaced by $\bar{a}(x)\, u(x) \equiv \Delta u(x)$, etc.

The cross sections Eqs. (29) and (33) can be used to estimate the weak asymmetries of Eqs. (15)–(17) at large $|\mathbf{Q}_\perp|$ for situations when valence quark interactions are apt to be dominant (e.g., πp collisions). Such estimates involve integrals of the functions $F_n(y, \delta)$; it is therefore convenient to introduce the notation

$$\begin{aligned} I_n(q, \bar{q}) &\equiv \iint dy_1\, dy_2\, q(x_1)\, \bar{q}(x_2)\, F_n(y_1, \delta)\{\delta(y_2 - y_2')\} \\ &= \int_{y_1,\min}^{y_1,\max} dy_1\, q(\tilde{x}_1 y_1)\, \bar{q}(\tilde{x}_2 y_2')\, F_n(y_1, \delta), \end{aligned} \tag{34a}$$

where the integrals are written in terms of $y_n = x_n/\tilde{x}_n$. It should be kept in mind that the functionals $I_n(q, \bar{q})$ also depend implicitly on the variables $\tilde{x}_1$, $\tilde{x}_2$ and δ. In particular,

$$I_1(q, \bar{q})|_{\tilde{x}_1, \tilde{x}_2} = I_2(\bar{s}, q)|_{\tilde{x}_1, \tilde{x}_2}. \tag{34b}$$

For quark/parton distributions identically equal to unity, the functional I_1 is given by

$$I_1(1, 1) = \frac{1+\delta}{\delta}\left\{\ln\left[\frac{(1-\tilde{x}_1)(1-\tilde{x}_2(1+\delta))}{\tilde{x}_1\delta}\right] - \left[1-(1+\delta)\tilde{x}_2 - \frac{\tilde{x}_1\delta}{1-\tilde{x}_1}\right]\right\}, \tag{35a}$$

which has the limit (see Eqs. (14))

$$I_1(1, 1) \to \frac{-\ln\delta}{\delta} + \frac{1}{\delta}\left\{\ln\left[\frac{(1-\bar{x}_1)(1-\bar{x}_2)}{\bar{x}_1}\right] - (1-\bar{x}_2)\right\} + \cdots \tag{35b}$$

as $\delta \to 0$. The functional $I_2(1, 1)$ is obtained by using Eq. (34b). Note also that as $\delta \to 0$, $I_1 \to I_2$. In fact, it can be shown that in general

$$\lim_{\delta\to 0}\begin{Bmatrix} I_1(q, \bar{q}) \\ I_2(q, \bar{q}) \end{Bmatrix} = \frac{-\ln\delta}{\delta}\left[q(\bar{x}_1)\,\bar{q}(\bar{x}_2)\right] + o\left(\frac{1}{\delta}\right), \tag{36}$$

so that

$$\lim_{\delta\to 0}\left[\frac{I_1(q, \bar{q}) - I_2(q, \bar{q})}{I_1(q, \bar{q}) + I_2(q, \bar{q})}\right] = o\left(\frac{1}{\ln\delta}\right). \tag{37}$$

With the use of the definitions

$$\begin{aligned} N(q, \bar{q}) &\equiv \zeta_1 I_1(q, \bar{q}) - \zeta_2 I_2(q, \bar{q}), \\ D(q, \bar{q}) &\equiv (1+\zeta_1^2) I_1(q, \bar{q}) + (1+\zeta_2^2) I_2(q, \bar{q}) \end{aligned} \tag{38}$$

the asymmetries Eqs. (15)–(17) are now calculated for $q\bar{q}$ annihilation processes. For πp collisions, the charge asymmetry at large $|\mathbf{Q}_\perp|$ is given by

$$\begin{Bmatrix} a_c^{\pi^- p}(l^+, l^-) \\ a_c^{\pi^+ p}(l^+, l^-) \end{Bmatrix} = \begin{Bmatrix} \dfrac{A_u}{(e_u/e)} & 2 & \dfrac{N(u_p, \bar{u}_\pi)}{D(u_p, \bar{u}_\pi)} \\ \dfrac{A_d}{(e_d/e)} & 2 & \dfrac{N(d_p, \bar{d}_\pi)}{D(d_p, \bar{d}^\pi)} \end{Bmatrix} \frac{A_l}{(e_l/e)} \frac{1}{2\pi\alpha} \frac{-Q^2}{Q^2 - M_Z^2} \tag{39a}$$

$$\simeq \begin{Bmatrix} -1.35 & \times 2 & \dfrac{N(u_p, \bar{u}_\pi)}{D(u_p, \bar{u}_\pi)} \\ -2.7 & \times 2 & \dfrac{N(d_p, \bar{d}_\pi)}{D(d_p, \bar{d}_\pi)} \end{Bmatrix} \times 10^{-4} \frac{Q^2}{(\mathrm{GeV})^2} \tag{39b}$$

to lowest order in Q^2/M_Z^2. The last line follows with $G_F = 1.17 \times 10^{-5}\ \mathrm{GeV}^{-2}$ and $\sin^2\theta_W = 0.225$. Note that the charge asymmetry is independent of the polarization of the initial hadrons. The (polarization-dependent) charge-helicity asymmetry at large $|\mathbf{Q}_\perp|$ can also be expressed in this notation. It is given by

$$\left.\begin{matrix} a_{\mathrm{ch}}^{\pi^- p}(l^+, l^-) \\ a_{\mathrm{ch}}^{\pi^+ p}(l^+, l^-) \end{matrix}\right\} = \left\{\begin{matrix} \dfrac{V_u}{(e_u/e)} & \dfrac{2N(\bar{\alpha}^u p, \bar{u}_\pi)}{D(u_p, \bar{u}_\pi)} \\ \dfrac{V_d}{(e_d/e)} & \dfrac{2N(\bar{\beta} d_p, \bar{d}_\pi)}{D(d_p, \bar{d}_\pi)} \end{matrix}\right\} \frac{A_l}{(e_l/e)} \frac{1}{2\pi\alpha} \left(\frac{-Q^2}{Q^2 - M_Z^2}\right) \tag{40a}$$

$$\simeq \left\{\begin{matrix} 5.5 & \dfrac{2N(\bar{\alpha} u_p, \bar{u}_\pi)}{D(u_p, \bar{u}_\pi)} \\ 9.5 & \dfrac{2N(\bar{\beta} d_p, \bar{d}_\pi)}{D(d_p, \bar{d}_\pi)} \end{matrix}\right\} \times 10^{-5} \frac{Q^2}{(\mathrm{GeV})^2} \tag{40b}$$

to lowest order in Q^2/M_Z^2. Finally, the helicity asymmetry at large $|\mathbf{Q}_\perp|$ is given by

$$\left.\begin{matrix} a_h^{\pi^- p}(l^+, l^-) \\ a_n^{\pi^+ p}(l^+, l^-) \end{matrix}\right\} = \left\{\begin{matrix} \dfrac{A_u}{(e_u/e)} & \dfrac{D(\bar{\alpha} u_p, \bar{u}_\pi)}{D(u_p, \bar{u}_\pi)} \\ \dfrac{A_d}{(e_d/e)} & \dfrac{D(\beta d_p, \bar{d}_\pi)}{D(d_p, d_\pi)} \end{matrix}\right\} \frac{V_l}{(e_l/e)} \frac{1}{2\pi\alpha} \frac{-Q^2}{Q^2 - M_Z^2} \tag{41a}$$

$$\simeq \left\{\begin{matrix} 1.4 & \dfrac{D(\bar{\alpha} u_p, \bar{u}_\pi)}{D(u_p, u_\pi)} \\ 2.8 & \dfrac{D(\bar{\beta} d_p, \bar{d}_\pi)}{D(d_p, \bar{d}_\pi)} \end{matrix}\right\} \times 10^{-5} \frac{Q^2}{(\mathrm{GeV})^2} \tag{41b}$$

to lowest order in Q^2/M_Z^2. Note that by Eq. (36) all three asymmetries Eqs. (39), (40), (41) approach their parton model equivalents Eqs. (17b), (21), and (20), respectively, in the limit $\delta \to 0$. In this limit $Q^2 \gg |\mathbf{Q}_\perp| \gtrsim (0.5\ \mathrm{GeV})^2$, where the second inequality follows from the requirement that the (nonperturbative) effects of the initial transverse momentum of the quark be negligible, as discussed previously.

The charge asymmetry for $\pi^- p$ collisions is plotted in Fig. 8 for typical parameter values ($\tau = 0.1$, $x_F = 0$, $\cos\theta_l = 1$, $\cos\phi_l = 1$, $\delta = 0.01$). The corresponding result for $\pi^+ p$ collisions is similar. The asymmetry at large $|\mathbf{Q}_\perp|$ is nearly equal to the ($|\mathbf{Q}_\perp| = 0$) parton model result (plotted in the same figure) for modes values of δ.

In order to evaluate the parity-violating asymmetries, models for the functions $\bar{\alpha}(x)$ and $\bar{\beta}(x)$ are needed. Consider the simple form

$$\alpha(x) = a x^p. \tag{42}$$

The boundary condition $\lim_{x\to 1} \bar{\alpha}(x) = 1$ (or $a = 1$) is suggested by perturbative QCD calculations [26] which indicate that a quark at $x = 1$ carries the spin of the parent

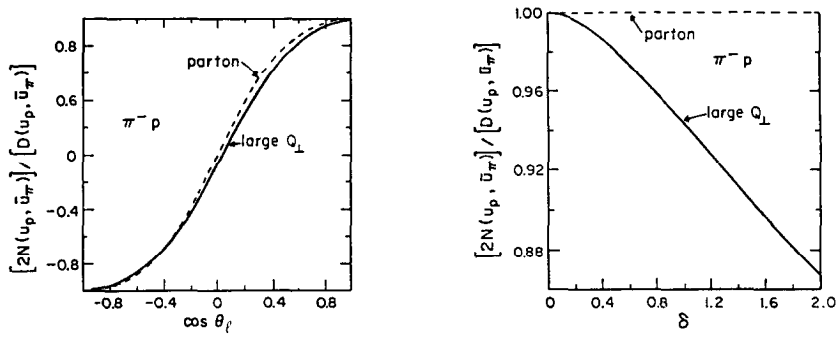

FIG. 8. (a) The solid line is a plot of $2N(u_p, \bar{u}_\pi)/D(u_p, \bar{u}_\pi)$ (the charge asymmetry for $\pi^- p$ collisions from Eq. (39)) versus $\cos\theta_l$. The other parameter values are $\tau = 0.1$, $x_F = 0$, $-\cos\phi_l = 1$, $\delta = 0.1$. The dashed line is the parton model ($\delta \to 0$) limit of this ratio, and is given analytically by $2\cos\chi/(1+\cos^2\chi)$. (b) The $\pi^- p$ charge asymmetry plotted as a function of δ for $\cos\theta_l = 1$, $\cos\phi_l = 1$, $\tau = 0.1$, $x_F = 0$. Note that the charge asymmetry varies little with δ. As pictured, the corresponding parton model result is simply unity.

proton. This simple form for $\bar{\alpha}(x)$ allows a solution of the sum rule Eq. (22a) in terms of a moment of the quark distribution and yields [28] $p \cong 0.39$.

Figure 9 shows the charge-helicity asymmetry for $\pi^- p$ collisions evaluated using the typical parameters of Fig. 8. Again, the asymmetry is nearly equal to the parton model result, Eq. (21).

Figure 10 shows the charge-helicity asymmetry valuated for $\pi^+ p$ collisions at large $|\mathbf{Q}_\perp|$. The choices of $\bar{\beta}(x)$ are used. Explicitly, these choices are

$$\bar{\beta}_{\rm I}(x) = -\tfrac{1}{3}x^q + \tfrac{4}{3}x^r, \tag{43a}$$

$$\bar{\beta}_{\rm II}(x) = -\tfrac{1}{3}x^{q'} \tag{43b}$$

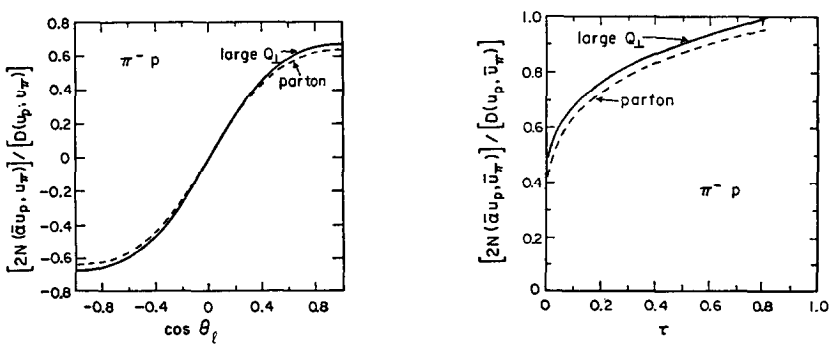

FIG. 9. (a) The solid line is a plot of $2N(\bar{\alpha}u_p, \bar{u}_\pi)/D(u_p, \bar{u}_\pi)$ (the charge-helicity asymmetry for $\pi^- p$ collisions from Eqs. (4)) versus $\cos\theta_l$. The other parameter values are $\tau = 0.1$, $x_F = 0$, $\cos\phi_l = 1$, $\delta = 0.1$. The dashed line is the parton model ($\delta \to 0$) limit of this ratio, and is given analytically by $\bar{\alpha}(\bar{x}_1) \cdot 2\cos\chi/(1+\cos^2\chi)$. (b) The solid line is a plot of the $\pi^- p$ charge-helicity asymmetry versus τ. The other parameters are as for (9a), and $\cos\theta_l = 1$. The dashed line is the corresponding parton model limit. Note that kinematics (specifically $y_{1,\min} < y_{1,\max}$ requires $\tau < (\sqrt{1+\delta} - \sqrt{\delta})^2$ for $x_F = 0$.

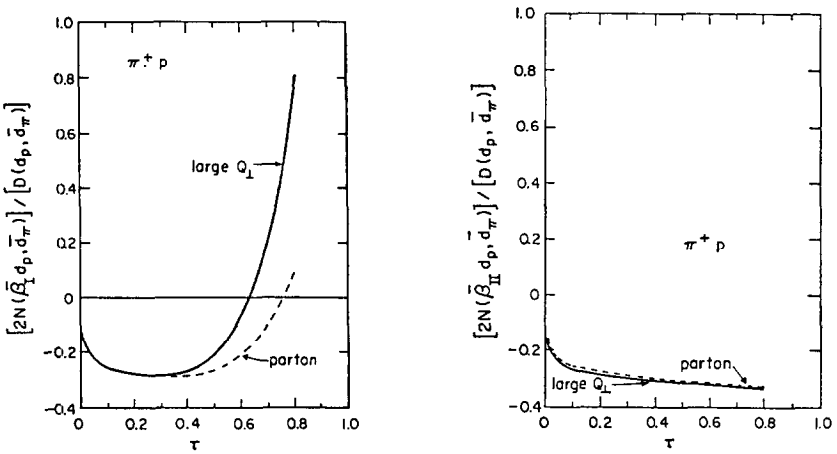

FIG. 10. (a) The solid line is a plot of $2N(\bar{\beta}_I d_p, \bar{d}_\pi)/D(d_p, \bar{d}_\pi)$ (i.e., the $\pi^+ p$ charge-helicity asymmetry of Eqs. (40)) versus τ for $\cos\theta_l = 1$, $\cos\phi_l = 1$, $x_\perp = 0$, $\delta = 0.01$. The broken line is a plot of the corresponding parton model result $\bar{\beta}_I(\bar{x}_2) \cdot 2\cos\chi/(1+\cos^2\chi)$. (b) The same as (a), but with $\bar{\beta}_{II}(x)$ substituted for $\bar{\beta}_I(x)$.

with $q \simeq q' \simeq 0.23$ and $r = 10$. The first choice is as suggested in Ref. [13], with the boundary condition as $x \to 1$ chosen so that a d quark at $x = 1$ carries the spin of the proton. In contrast to the situation for the polarized u-quark, the uu pair left at $x = 0$ would have isospin and spin 1. Nevertheless calculations [26] based on perturbative QCD suggest that this situation does indeed occur. This boundary condition and the sum rule Eq. (22b) imply that $\bar{\beta}(x)$ changes sign at some value of x.

The choice $\bar{\beta}_{II}(x)$ is as suggested in Ref. [22], with the boundary condition as $x \to 1$ chosen so that $\bar{\beta}_{II}(x)$ reproduces the $SU(6)$ result in the limit. No sign change is implied at any x for this choice.

The power $q = 0.23$ in Eq. (43a) is chosen to satisfy the sum rule Eq. (22b). The power $r = 10$ is chosen essentially arbitrarily; because r is large the second term in Eq. (43a) makes only a negligible contribution to the sum rule Eq. (22b). Thus, $q' \simeq q = 0.23$ as well.

As can be seen from Fig. 10a, the $\pi^+ p$ charge-helicity asymmetry at large $|\mathbf{Q}_\perp|$ calculated using the function $\beta_I(x)$ changes sign at a value of τ slightly less than the value for which the $|\mathbf{Q}_\perp| = 0$ parton model result changes sign. Numerically the two results are otherwise quite similar, except for τ near unity.

Figure 11 shows the helicity asymmetry for $\pi^- p$ and $\pi^+ p$ collisions. In the case of $\pi^- p$ collisions, the large $|\mathbf{Q}_\perp|$ result is quite similar to the parton model calculation. However for $\pi^+ p$ collisions, as in the case of the charge-helicity asymmetry, the sign change associated with the d quark polarization distribution $\beta_I(x)$ occurs at a smaller value of τ than for the parton model result.

Though for πp collisions the contributions of initial gluon processes are numerically negligible [10, 11], for pp collisions they are not. This difference occurs because $q\bar{q}$ annihilation processes in pp collisions require a sea antiquark and are

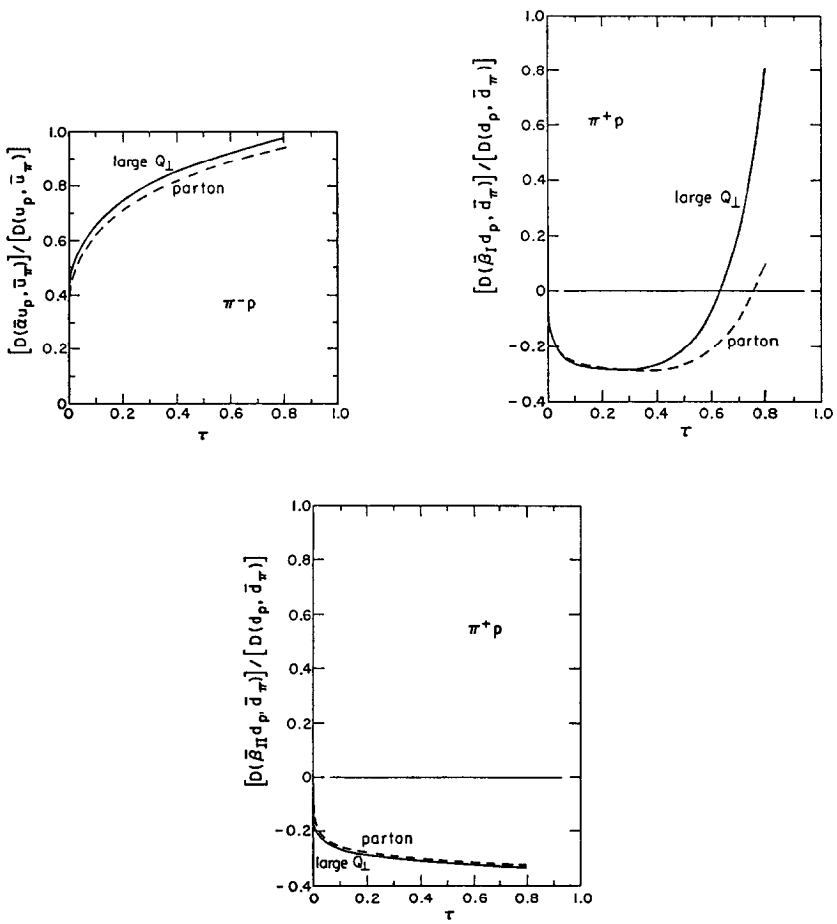

FIG. 11. (a) The solid line is a plot of $D(\bar{a}u_p, \bar{u}_\pi)/D(u_p, \bar{u}_\pi)$ (i.e. the $\pi^- p$ helicity asymmetry of Eqs.)41)) versus τ for $\cos\theta_l = 1$, $\cos\phi_l = 1$, $x_F = 0$, $\delta = 0.01$. The broken line is a plot of the corresponding parton model result $\bar{a}(\bar{x}_1)$. (b) The solid line is a plot of $D(\bar{\beta}_1 d_p, \bar{d}_\pi)/D(d_p, \bar{d}_\pi)$ (i.e. the $\pi^+ p$ helicity asymmetry of Eq. (41)). The other parameter values are as in (a). The broken line is the corresponding parton model result $\bar{\beta}_1(\bar{x}_1)$. (c) As in (b), but for β_{II} instead of β_1.

thus suppressed. In order to analyze *pp* collisions initial gluon processes are now considered.

2. *Initial gluon diagrams*

(a) ELECTROMAGNETIC CROSS SECTION. The matrix element for the initial gluon diagrams Figs. 2c and d and Figs. 5c and d can be obtained from the corresponding final gluon by crossing symmetry. To obtain the squared initial gluon matrix element from the squared final gluon matrix element Eq. (24) multiply by -1

(because of the antiquark projection operator) and redefine the propagator variables k' and k'' as follows:

$$\text{initial gluon} \begin{cases} k' \equiv Q_\mu + p'_\mu + k_\mu, & \text{(44a)} \\ k'' \equiv p_\mu - Q_\mu. & \text{(44b)} \end{cases}$$

The parton model is introduced via the substitution:

$$p^\mu = x_1 P_1^\mu, \tag{45a}$$

$$k^\mu = x_2 P_2^\mu, \tag{45b}$$

where P_1^μ and P_2^μ are the four-momenta of the incoming hadrons as in Eqs. (26b) and (26c). The variables are x_1, y_1, x_2, y_2, and remain as defined by Eqs. (27). The electromagnetic cross section for lepton pair production from hadron–polarized hadron collisions via the initial gluon mechanism is

$$\begin{aligned} d\sigma^{\mathrm{EM}}(qG) = & \left(\frac{1}{6}\frac{\alpha_s}{2\pi}\right)\left(\frac{e_q}{e}\right)^2\left(\frac{e_l}{e}\right)^2 \frac{\alpha^2}{2\pi} q(x_1)\, G(x_2) \\ & \times \delta(y_2 - y_2')\, dx_1\, dx_2 \frac{1}{(Q^2)^2} \frac{d^3Q d^3l}{Q_0^2 - l_0^2} \\ & \times \left[(1+\zeta_1^2) F_3(y_3(y_1,\delta) + \left(1 - \zeta_1\zeta_2 - \frac{2\delta}{1+\delta}\right) F_4(y_1,\delta)\right. \\ & \left. + (1+\zeta_2^2) F_5(y_1,\delta)\right], \end{aligned} \tag{45c}$$

where

$$F_3(y_1,\delta) \equiv -2(1+\delta)\frac{y_1 - (1+\delta)}{(y_1-1)^3} = \frac{2(1+\delta)^2}{y_2'(y_1-1)}, \tag{46a}$$

$$F_4(y_1,\delta) \equiv \frac{2(1+\delta)^2}{y_1(y_1-1)^2}, \tag{46b}$$

$$F_5(y_1,\delta) \equiv \frac{(1+\delta)^3}{y_1^2(y_1-1)[y_1-(1+\delta)]} = \frac{y_2'(1+\delta)^2}{y_1^2(y_1-1)^2} \tag{46c}$$

and $G(x_2)$ denotes the distribution of gluons in momentum fraction x_2. The color factor of $1/6$ is calculated from the λ matrices of the ($SU(3)$) color group by

$$\frac{1}{6} = \frac{1}{3}\cdot\frac{1}{8}\sum_i \mathrm{Tr}\left(\frac{1}{2}\lambda_i \frac{1}{2}\lambda_i\right). \tag{47}$$

In the limit $\delta \to 0$, the functionals I_3, I_4 and I_5 approach the limits

$$I_3(q, G) \to \frac{1}{\delta} q(\bar{x}_1)\, G(\bar{x}_2)\, \frac{1-2\bar{x}_1}{(1-\bar{x}_2)^2}, \tag{48a}$$

$$I_4(q, G) \to \frac{1}{\delta} q(\bar{x}_1)\, G(\bar{x}_2) - \frac{2}{1-\bar{x}_2}, \tag{48b}$$

$$I_5(q, G) \to \frac{1}{\delta} q(\bar{x}_1)\, G(\bar{x}_2) \ln \bar{x}_2. \tag{48c}$$

Equations (48) imply that the initial gluon contributions to the differential lepton pair production cross section are of order $1/\delta$, to be compared with the $\ln \delta/\delta$ contributions from final gluon graphs. The quark–antiquark annihilation processes must therefore dominate the initial gluon processes for sufficiently small δ.

The reason for the factor of $\ln \delta/\delta = \frac{1}{2}d(\ln^2 \delta)/d\delta$ in the annihilation cross section compared to a term of order $1/\delta = d(\ln \delta)/d\delta$ in the initial gluon cross section comes from kinematic considerations. Consider Eqs. (24) and (32). For the annihilation process both k'^2/Q^2 and k''^2/Q^2 are of order δ for small δ; however in the initial gluon processes k'^2 is bounded below by Q^2. Thus the squared matrix element calculated from the initial gluon graphs is less singular than the one calculated from the annihilation graphs as $\delta \to 0$.

(b) ELECTROWEAK CROSS SECTION. For the purposes of this calculation, it is assumed that gluons do not carry a significant fraction of the proton spin.[2] The calculation of the electroweak gluon–polarized quark contribution to the hadron–polarized hadron lepton pair production cross section is then straightforward. The result is

$$\begin{aligned} d\sigma^{\mathrm{EW}}(qG) = \frac{1}{6}\frac{\alpha_s}{2\pi}\left(\frac{e_q}{e}\right)\left(\frac{e_l}{e}\right)\alpha \cdot \frac{1}{2\pi^2}\frac{1}{(Q^2)^2(Q^2-M_Z^2)}\frac{d^3l d^3Q}{Q_0^2 - l_0^2}\, dx_1\, dx_2 \\ \times G(x_2)\Big\{ V_l[V_q q(x) - A_q \Delta q(x)]\Big[(1+\zeta_1^2)F_3(y_1,\delta) \\ + \left(1 - \zeta_1\zeta_2 - \frac{2\delta}{1+\delta}\right)F_4(y_1,\delta) + (1+\zeta_2^2)F_5(y_1,\delta)\Big] \\ + A_l[A_q q(x_1) - V_q \Delta q(x_1)]\Big[\zeta_1 F_6(y_1,\delta) - \zeta_2 F_7(y_1,\delta)\Big]\Big\}, \end{aligned} \tag{49}$$

where $G(x)$ is the appropriate gluon distribution and

$$F_6(y_1, \delta) = -(1+\delta)^2\left[\frac{2\delta}{1+\delta}\frac{1}{(y_1-1)^2} - \frac{1}{(y_1-1)^2} - \frac{1}{y_1}\right], \tag{50a}$$

[2] There is as yet no experimental evidence for gluon polarization in protons.

$$F_7(y_1,\delta)=-(1+\delta)\left[\frac{1+\delta}{(y_1-1)^2}+\frac{(1+2\delta)(1+\delta)}{\delta}\frac{1}{y_1-1}\right.$$
$$\left.-\frac{1}{\delta}\frac{1}{y_1-(1+\delta)}+\frac{1+2\delta}{y_1}+\frac{1+\delta}{y_1^2}\right]. \tag{50b}$$

As $\delta\to 0$ the corresponding functionals I_n approach the limits

$$I_6(q,G)\to\frac{-1}{\delta}\cdot q(\bar{x}_1)\,G(\bar{x}_2)\cdot\bar{x}_2(1-\bar{x}_2), \tag{51a}$$

$$I_7(q,G)\to\frac{-1}{\delta}\cdot q(\bar{x}_1)\,G(\bar{x}_2)(1-\bar{x}_2+\ln\bar{x}_2). \tag{51b}$$

Thus as $\delta\to 0$, the electroweak contribution to the cross section Eq. (49) is proportional to $1/\delta$. This result follows from kinematics, as discussed previously.

These results for the initial gluon processes can be used to calculate the weak asymmetries at large $|\mathbf{Q}_\perp|$ in proton–proton collisions. These results are presented in the form (to lowest order in Q^2/M_Z^2):

$$a_c^{pp}=\frac{A_u}{(e_u/e)}\frac{A_l}{(e_l/e)}\frac{1}{2\pi\alpha}\frac{Q^2}{M_Z^2}\Phi_c(pp)$$
$$\sim -1.35\times 10^{-4}\frac{Q^2}{(\mathrm{GeV})^2}\Phi_c(pp), \tag{52a}$$

$$a_{\mathrm{ch}}^{pp}=\frac{V_u}{(e_u/e)}\frac{A_l}{(e_l/e)}\frac{1}{2\pi\alpha}\frac{Q^2}{M_Z^2}\Phi_{\mathrm{ch}}^{(pp)}$$
$$\sim 5.5\times 10^{-5}\frac{Q^2}{(\mathrm{GeV})^2}\Phi_{\mathrm{ch}}^{(pp)}, \tag{52b}$$

$$a_h^{pp}=\frac{A_u}{(e_u/e)}\frac{V_l}{(e_l/e)}\frac{1}{2\pi\alpha}\frac{Q^2}{M_Z^2}\Phi_h^{(pp)}$$
$$\sim 1.4\times 10^{-5}\frac{Q^2}{(\mathrm{GeV})^2}\Phi_h^{(pp)}. \tag{52c}$$

To first order in the weak interaction the functions consist of the ratio of an electroweak interference "numerator" and a pure electromagnetic "denominator." Each function consists of contributions from annihilation and initial gluon cross sections summed over all quark and antiquark types. The result is normalized to an "effective" u quark cross section. For example, the denominator of each Φ is given by

$$\frac{1}{e_u^2}\left[\sum_{q,\bar{q}}d\sigma^{\mathrm{EM}}(q\bar{q})+\sum_{q}d\sigma^{\mathrm{EM}}(qG)+\sum_{\bar{q}}d\sigma^{\mathrm{EM}}(\bar{q}G)\right]. \tag{53}$$

Similarly, the numerator of, e.g., $\Phi_c(pp)$ is given by

$$\frac{1}{(A_u e_u)}\left[\sum_{q\bar{q}} d\sigma_c^{EW}(q\bar{q}) + \sum_{q} d\sigma_c^{EW}(qG) + \sum_{\bar{q}} d\sigma_c^{EW}(\bar{q}G)\right]. \tag{54}$$

The notation $d\sigma_c^{EW}$ refers to the parity-conserving charge-antisymmetric portion of the electroweak interference cross section, i.e., the portion involving the function $A_0(k', k'', Q, l)$ defined in Eq. (32b).

In Fig. 12a, $\Phi_c(pp)$ is plotted versus $\cos\theta_l$ for the typical parameter values used in Fig. 8. For this calculation, as before, $\sin^2\theta_W$ is taken to be 0.225. Figure 12b shows $\Phi_c(pp)$ plotted versus τ. In both cases, the resulting charge asymmetry at large $|\mathbf{Q}_\perp|$ is very similar to the parton model result. Also note that the symmetry of the initial (pp) state requires that the charge asymmetry vanish when the vector $\mathbf{Q}$ is normal to the hadron beam direction (i.e., when $x_F = 0$). The gluon distribution is taken to be

$$G(x) = \frac{n+1}{2}\frac{(1-x)^n}{x} \tag{55}$$

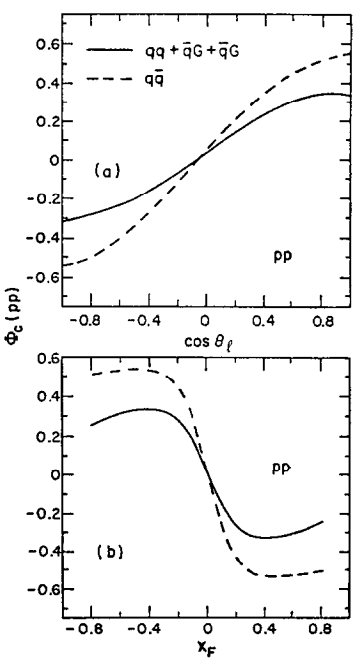

FIG. 12. (a) is a plot of $\Phi_c(pp)$ (i.e., the charge asymmetry for pp collisions) versus $\cos\theta_l$. In this calculation, $\sin^2\theta_W = 0.225$. The other parameters are $\tau = 0.1$, $\delta = 0.01$, $\cos\Phi_l = 1$, $x_F = 0.5$. The broken line is the result obtained from $q\bar{q}$ annihilation only; the solid line is the result with $q\bar{q}$ annihilation as well as qG and $\bar{q}G$ scattering. The gluon distribution parameter n of Eq. (55) is set equal to 5. (b) is a plot of $\Phi(pp)$ versus x_F for $\cos\Phi_l = 1$ with other parameters and definitions as in Fig. 14a.

with $n = 5$. This choice is motivated by simplicity and the empirical result that gluons carry roughly half the proton momentum at present energies,

Consider next the charge-helicity asymmetry for pp collisions. As discussed previously the $u\bar{u}$ and $d\bar{d}$ annihilation contributions to the electroweak interference are typically of opposite sign. In the analogous parton model calculation [13] this sign difference led to the consequence that if $\bar{u}(x)/\bar{d}(x) \to 0$ as $x \to 1$, then the parity-violating asymmetries change sign as a function of τ.

For the asymmetries at large $|\mathbf{Q}_\perp|$ an additional contribution comes from the graphs such as those in Figs. 2c and d where an initial gluon scatters with a quark (or antiquark, though this latter antiquark process is usually negligible).

The antiquark distributions used for the following calculations [18] are proportional to $(1-x)^7$ (for the $\bar{d}$ antiquarks) or higher powers of $(1-x)$ as $x \to 1$ for other flavors. Lore on gluon distributions [29] suggests forms like that of Eq. (55) with $n \simeq 5$–7. As x approaches 1, the initial gluon contribution to the cross section must dominate the quark–antiquark annihilation contribution if the gluon distribution is much larger than the antiquark distributions. Should this be the case, an $SU(2)$ flavor asymmetry of the form proposed in Ref. [18] need not cause a sign change in the asymmetries at large τ.

The pp charge helicity asymmetry for several values of the gluon distribution parameter n is plotted in Fig. 13. As indicated, no sign change occurs if $n \lesssim 7$ (the value of the $\bar{d}$ antiquark distribution parameter) for typical parameter values. Figure 14 displays the helicity asymmetry for several values of n; the same conclusion holds. A sign change observed in the parity-violating asymmetries in pp collisions as a function of τ would therefore suggest two things—first, that the gluon distribution falls more rapidly than the antiquark distributions as $x \to 1$; and second that the antiquark sea is flavor $SU(2)$ asymmetric in the fashion proposed in Ref. [18].

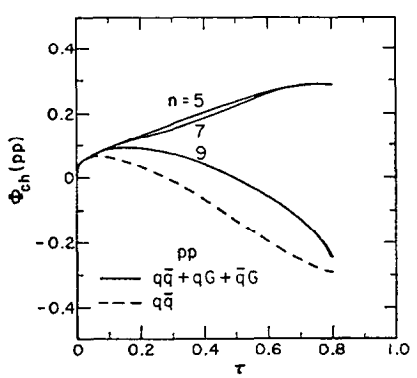

FIG. 13. Plots of $\Phi_{ch}(pp)$ (the proton–polarized proton charge-helicity asymmetry) versus τ. The other parameters are the same as for Fig. 12a, except $x_F = 0$. The broken line indicates the asymmetry resulting from quark–antiquark annihilation only, while the solid line displays the asymmetry with the contributions of initial gluon processes included. The polarization distribution for the d quark is $\bar{\beta}_{11}(x)$.

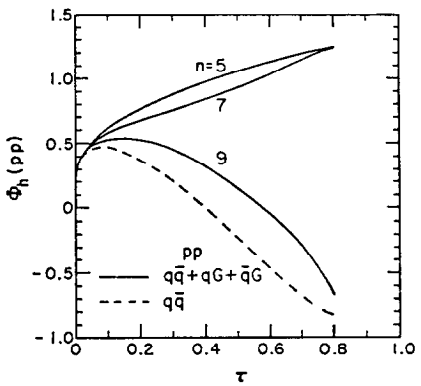

FIG. 14. The solid lines are plots of $\Phi_h(pp)$ (the proton–polarized proton helicity asymmetry) versus τ for several values of the gluon distribution parameter n of Eq. (55). The broken line indicates the asymmetry arising from quark–antiquark annihilation only. Other parameters and definitions are the same as for Fig. 13a.

C. *Weak Asymmetries in Integrated Cross Sections*

1. *Motivation*

In the preceding section various weak asymmetries were evaluated at fixed (presumably large) values of $|\mathbf{Q}_\perp|$. It was seen that the cross section for lepton pair production from massless quarks and gluons is finite provided $|\mathbf{Q}_\perp|$ is bounded away from zero.

Another finite quantity which can be calculated in this perturbative formalism is the cross sections integrated over transverse momentum [10] (referred to as the "integrated cross section"). The effects of the virtual gluon diagrams (such as Figs. 3 and 6) are included along with the effects of the real gluon graphs discussed in the previous section. In this section the incoming quarks and gluons are assumed to have no initial transverse momentum. Thus the virtual gluon graphs only give contributions to the differential cross section which are proportional to the singular function $\delta^2(\mathbf{Q}_\perp)$.

As shown in the previous section, the contributions of the real gluon graphs to the differential cross section diverge as $\ln \delta/\delta$ when $\delta = |\mathbf{Q}_\perp|^2/Q^2 \to 0$. Both the real and virtual gluon contributions to the integrated cross section are formally infinite in $n = 4$ space-time dimensions. However if the expression for the cross section is analytically continued to $n = 4 - 2\varepsilon$ dimensions (with $\varepsilon < 0$) the singular contributions appear as poles in ε when quark and gluon masses are set to zero [30, 31]. The most singular contributions are of order ε^{-2} and arise from the coincidence of the infrared and collinear singularities in both the real and virtual gluon diagrams. A second-order pole is equivalent to a $\ln^2(Q^2/M^2)$ singularity [10], where M is an infrared cutoff.

The coefficient of the second-order poles in the real and virtual gluon contributions are of equal magnitude and opposite sign. Therefore the most singular terms in the

sum of the real and virtual gluon contributions are of order ε^{-1}. These latter singularities are absorbed into the renormalized parton distributions [6–11]. At the end of the calculation, ε is set equal to zero. All (renormalized) final results are finite. This technique for isolating and removing singularities has come to be known as dimensional regularization [30, 31].

2. *Quark–Antiquark Annihilation Diagrams*

(a) ELECTROMAGNETIC CROSS SECTION. The squared matrix element for electromagnetic lepton pair production from quark–antiquark annihilation in $n = 4 - 2\varepsilon$ dimensions (i.e., the n-dimensional generalization of Eqs. (24)) is

$$\sum_{\text{real gluon}} |M_{\text{EM}}|^2 \, q\bar{q} = g_s^2(\mu^2)^{\varepsilon} e_l^2 e_q^2 S_{\varepsilon}(k', k'', Q, l), \tag{56a}$$

where

$$\begin{aligned} S_{\varepsilon}(k', k'', Q, l) = \frac{16Q^2}{k'^2 k''^2} \{ & [2Q^2(1-\varepsilon) + l^2] \, Q^2 \\ & + (l \cdot k')^2 + (l \cdot k'')^2 - \varepsilon [l \cdot (k' - k'')]^2 \} \\ & - \frac{8}{k'^2} [2Q^2(1-\varepsilon) + l^2][2Q^2 - (1-\varepsilon) k''^2] \\ & - \frac{8}{k''^2} [2Q^2(1-\varepsilon) + l^2][2Q^2 - (1-\varepsilon) k'^2] \end{aligned} \tag{56b}$$

and $l^2 = 4m_l^2 - Q^2 \simeq -Q^2$ are lepton masses are to be neglected. The (no longer dimensionless) quark–gluon coupling is written as the product of the usual dimensionless coupling g_s and a scale factor μ^{ε} which approaches unity as n-approaches 4 (i.e., as $\varepsilon \to 0$).

The calculation of this squared matrix element involves the contraction of the lepton tensor

$$L_{\mu\nu} \sim (Q^2 g_{\mu\nu} - Q_\mu Q_\nu) + l_\mu l_\nu \tag{57}$$

with a similar hadronic tensor. The lepton tensor consists of two distinct terms. The first term, marked with parentheses in Eq. (57), is simply the transverse projection operator for a massive virtual photon of four-momentum Q_μ. Thus the cross section for producing such a massive virtual photon can be recovered from the lepton pair production cross section presented here by taking the limit $l_\mu \to 0$.

Note that in this limit the squared matrix element Eqs. (56) is proportional to $(1 - \varepsilon)$ and thus vanishes in two dimensions where $\varepsilon = 1$. This consequence is in accord with the fact that two dimensions are not sufficient to allow transversely polarized photons to be produced.

Choosing the right variables in order to perform the dimensional regularization is very important. The variables used for this calculation,

$$q\bar{q}\ \text{annihilation}\begin{cases} y \equiv \dfrac{k'^2}{k'^2 + k''^2} \quad (1-y) = \dfrac{k''^2}{k'^2 + k''^2}, & \text{(58a)} \\ z \equiv \dfrac{Q^2}{Q^2 - k'^2 - k''^2} = \dfrac{\tau}{x_1 x_2}, & \text{(58b)} \end{cases}$$

allow the expressions for the matrix element and phase space to be simplified considerably. In addition, to facilitate the comparison with the work of Ref. [10] the following variables are defined:

$$q\bar{q}\ \text{annihilation}\begin{cases} y^* \equiv \dfrac{(x_2 - \bar{x}_2)(\bar{x}_1 + x_2)}{x_2(1-z)(x_1 + x_2)} \\ \quad = \dfrac{x_2 - x_1 z + x_F}{(1-z)(x_1 + x_2)}, & \text{(58c)} \\ 1 - y^* = \dfrac{(x_1 - \bar{x}_1)(x_1 + \bar{x}_2)}{x_1(1-z)(x_1 + x_2)} \\ \quad = \dfrac{x_1 - x_2 z + x_F}{(1-z)(x_1 + x_2)}. & \text{(58d)} \end{cases}$$

The variables Eqs. (58) have the bounds

$$0 < y < 1, \tag{59a}$$

$$\tau < z < 1 \tag{59b}$$

which follow from the kinematic limits

$$Q^2 - s < k'^2, \qquad k''^2 < 0. \tag{60}$$

The variable y has the physical interpretation

$$y = \cos^2 \frac{\theta_Q}{2} \tag{61}$$

in the hadron c.m. frame. The variable θ_Q is the angle between the vector $\mathbf{Q}$ and the z axis.

The n-dimensional phase space for the $q\bar{q}$ annihilation process is defined for massless particles by

$$\int (\text{P.S.}) \equiv \iiint \frac{d^n k}{(2\pi)^n} [2\pi\delta^+(k^2)] \frac{d^n l^+}{(2\pi)^n} [2\pi\delta^+(l^{+2})]$$

$$\times \frac{d^n l^-}{(2\pi)^n} [2\pi\delta^+(l^{-2})](2\pi)^n \delta^n(p + p' - k - l^+ + l^-) \tag{62a}$$

with

$$\delta^+(k^2) \equiv \theta(k_0)\,\delta(k^2), \qquad \text{etc.} \tag{62b}$$

Rewriting Eq. (62a) in terms of the variables Eq. (58) yields

$$\int (\text{P.S.}) = \frac{1}{16\pi}\frac{Q_0}{Q_0^2 - l_0^2}\left(\frac{4\pi}{Q^2}\right)^{\varepsilon}\frac{1}{\Gamma(1-\varepsilon)}\,dx_F\left\{\frac{d^{n-1}l}{(2\pi)^{n-1}}\right\}$$

$$\times z^{\varepsilon}(1-z)^{1-2\varepsilon}\int dy[y(1-y)]^{-\varepsilon}$$

$$\times \delta[(x_1+x_2)(1-z)y + x_1 z - x_2 - x_F]. \tag{63}$$

In the above relation, the integrations over the $n-3$ spurious azimuthal angles have been performed [30, 31]. The four-vector l does not appear in the energy-momentum conserving delta function $\delta^{(n)}(p+p'-k-l^+-l^-)$ in Eq. (62a), nor in the propagator variables k' and k''. Therefore the dimensional regularization does not affect the l integration and n may be immediately set equal to 4 in the expression in curly brackets in Eq. (63). The cross section for lepton pair production via the diagrams of Figs. 2a and b (which involve contributions of order ε^{-2} and ε^{-1}) is

$$d\sigma^{\text{EM}}_{\text{real gluon}}(q\bar{q}) = \left[\frac{4}{9}\frac{\alpha_s}{2\pi}(\mu^2)^{\varepsilon}\right]\left(\frac{e_q}{e}\right)^2\left(\frac{e_l}{e}\right)^2\alpha^2\frac{8\pi^4}{(Q^2)^2 s}$$

$$\times \int (\text{P.S.})\int\frac{dx_1}{x_1}\int\frac{dx_2}{x_2}\,S_{\varepsilon}(k', k'', Q, l)\,q(x_1)\,\bar{q}(x_2) \tag{64}$$

including the color factor 4/9.

The variables defined in Eqs. (58) are substituted into the squared matrix element Eq. (58). When multiplied by the regulating phase space factors in Eq. (63) the squared matrix element can be expanded in a power series in ε for small ε by using the well-known device [32]:

$$\int_0^1\frac{h(t)}{t^{(1+\varepsilon)}}\,dt = \int_0^1\frac{h(t)-h(0)}{t(1+\varepsilon)}\,dt + h(0)\int_0^1\frac{dt}{t^{1+\varepsilon}} \tag{65a}$$

$$= -\frac{1}{\varepsilon}h(0) + \int_0^1\frac{h(t)-h(0)}{t}\,dt$$

$$-\varepsilon\int_0^1\frac{\ln t}{t}[h(t)-h(0)]\,dt + o(\varepsilon^2). \tag{65b}$$

The definition

$$\int_0^1\frac{h(t)}{t_+}\,dt \equiv \int_0^1\frac{h(t)-h(0)}{t}\,dt \tag{65c}$$

is employed for an arbitrary test function $h(t)$. It follows from Eqs. (65) that

$$\frac{1}{t^{(1+\varepsilon)}} = -\frac{1}{\varepsilon}\,\delta(t) + \frac{1}{t_+} - \varepsilon\left(\frac{\ln(t)}{t}\right) + o(\varepsilon^2). \tag{66}$$

The method of Eq. (66) is used to obtain

$$\begin{aligned}
&\frac{1}{Q^2}\, z^{\varepsilon}(1-z)^{1-2\varepsilon}[y(1-y)]^{-\varepsilon} S_{\varepsilon}(k', k'', Q, l) \\
&\quad = \frac{1}{2}\left\{\frac{1}{\varepsilon^2}\,\delta(1-z)[\delta(y)+\delta(1-y)] - \frac{1}{\varepsilon}\,\delta(1-z)\left[\frac{1}{y_+} + \frac{1}{(1-y)_+}\right]\right. \\
&\qquad \left. + \delta(1-z)\left(\frac{\ln(1-y)}{y} + \frac{\ln y}{1-y} + \left(\frac{\ln(1-y)}{1-y}\right)_+ + \left(\frac{\ln y}{y}\right)_+\right)\right\} \\
&\qquad \times \left[1 + \frac{1}{2}\,\frac{l^2}{Q^2} + \frac{(l+k')^2 + (l\cdot k'')^2}{(Q^2)^2}\right] \\
&\qquad + \left\{\frac{-1}{\varepsilon}\,[\delta(y)+\delta(1-y)] + \frac{1}{y_+} + \frac{1}{(1-y)_+}\right\} \\
&\qquad \times \left\{\left[\left(1 + \frac{1}{2}\,\frac{l^2}{Q^2}\right)\frac{1}{2}\,\frac{1+z^2}{(1-z)_+} + \left[\frac{(l\cdot k')^2 + (l\cdot k'')^2}{(Q^2)^2}\right]\frac{z^2}{(1-z)_+}\right.\right. \\
&\qquad \left.\left. + \frac{1}{2}\,\delta(1-z)\left(1 + \frac{[l\cdot(k'-k'')]^2}{(Q^2)^2}\right)\right\} + [\delta(y)+\delta(1-y)]\right. \\
&\qquad \times \left(\left\{\frac{-\ln z}{1-z} + 2\left[\frac{\ln(1-z)}{1-z}\right]_+\right\}\left[\left(1 + \frac{1}{2}\,\frac{l^2}{Q^2}\right)\frac{1}{2}\,(1+z^2)\right.\right. \\
&\qquad + \frac{(l\cdot k')^2 + (l\cdot k'')^2}{(Q^2)^2}\, z^2 + \frac{1}{2}\,\frac{1+z^2}{(1-z)_+} + \left(1 + \frac{1}{2}\,\frac{l^2}{Q^2}\right)\frac{(1-z)}{2} \\
&\qquad \left.\left. + \frac{[l\cdot(k'-k'')]^2}{(Q^2)^2}\,\frac{z^2}{(1-z)_+}\right) - \left(1 + \frac{1}{2}\,\frac{l^2}{Q^2}\right)(1-z) + o(\varepsilon)\right.
\end{aligned} \tag{67}$$

which reduces to an expression derived elsewhere [10] times a factor $(1-\varepsilon)$ in the limit $l_\mu \to 0$. The integration over y is performed with the use of the identities

$$\int_0^1 \frac{dy}{y_+} = \int_0^1 \frac{dy}{(1-y)_+} = 0, \tag{68a}$$

$$\int_0^1 \frac{\ln y}{1-y}\,dy = \int_0^1 \frac{\ln(1-y)}{y}\,dy = \frac{-\pi^2}{6}. \tag{68b}$$

The contribution to the electromagnetic cross section from the virtual diagrams Figs. 3 can be obtained by multiplying the n-dimensional Drell–Yan (Fig. 1) cross section

$$d\sigma^{\mathrm{EM}}_{\text{parton}}(q\bar{q}) = \frac{1}{3}\left(\frac{e_l}{e}\right)^2\left(\frac{e_q}{e}\right)^2\frac{\alpha^2}{(Q^2)^2}\left(\frac{1}{2}\frac{|l|^3}{-l^2Q_0}\right)d^2\Omega_l\,dQ^2\,dx_F\,q(\bar{x}_1)\,\bar{q}(\bar{x}_2)$$
$$\times\,\delta(1-z)\,\delta(x_1-x_2+x_F)\frac{dx_1\,dx_2}{x_1x_2}\left(1-\varepsilon+\frac{1}{2}\frac{l^2}{Q^2}\sin^2\chi\right) \tag{69}$$

(which includes a color factor of 1/3) by a factor Γ, where Γ is defined via the real part of the photon vertex function with one gluon loop corrections. This order α_s vertex function is [10, 31]

$$\mathrm{Re}\,\Gamma^\mu(Q^2) \equiv \gamma^\mu(1+\Gamma) = \gamma^\mu\left[1+\left(\frac{4}{3}\frac{\alpha_s}{4\pi}\right)\left(\frac{4\pi\mu^2}{Q^2}\right)^\varepsilon\right. \tag{70a}$$
$$\left.\times\frac{\Gamma(1+\varepsilon)\,\Gamma(1-\varepsilon)}{\Gamma(1-2\varepsilon)}\left(\frac{-2}{\varepsilon^2}-\frac{3}{\varepsilon}-8+\pi^2\right)\right]. \tag{70b}$$

When the integrated real and virtual gluon contributions are added, the terms proportional to ε^{-2} cancel. The leading term in the sum is of order $1/\varepsilon$; this sum is given by

$$d\sigma^{\mathrm{EM}}_{\text{unrenormalized}}(q\bar{q})$$
$$= d\sigma^{\mathrm{EM}}_{\substack{\text{virtual}\\\text{gluon}}}(q\bar{q}) + d\sigma^{\mathrm{EM}}_{\substack{\text{real}\\\text{gluon}}}(q\bar{q})$$
$$= 2\left(\frac{e_q}{e}\right)^2\left(\frac{e_l}{e}\right)^2\left(\frac{4}{3}\frac{\alpha_s}{2\pi}\right)\left(\frac{4\pi\mu^2}{Q^2}\right)^\varepsilon\frac{\alpha^2}{(Q^2)^2s}$$
$$\times\frac{q(x_1)\,\bar{q}(x_2)}{\Gamma(1-\varepsilon)}\frac{dx_1}{x_1}\frac{dx_2}{x_2}\,d^2\Omega_l\,dQ^2\,dx_F$$
$$\times\frac{1}{2}Q^2\left(\frac{-1}{l^2}\left(\frac{Q^2}{Q^2+\frac{1}{4}x_F^2s\cos^2\theta_l}\right)^{3/2}(Q^2+\tfrac{1}{4}x_F^2s)\right.$$
$$\times\left\{\frac{-3}{4\varepsilon}P_{qq}(z)\left(1+\frac{1}{2}\frac{l^2}{Q^2}\sin^2\chi\right)[\delta(x_1z-x_2-x_F)+\delta(x_2z-x_1+x_F)]\right.$$
$$+\left[\frac{1}{2}\left(\frac{2}{3}\pi^2-8\right)\left(1+\frac{1}{2}\frac{l^2}{Q^2}\sin^2\chi\right)+\frac{3}{2}\right]\delta(1-z)\,\delta(x_1-x_2+x_F)$$
$$+[\delta(x_1z-x_2-x_F)+\delta(x_2z-x_1+x_F)]\left\{\left[\frac{-\ln z}{1-z}+2\left(\frac{\ln(1-z)}{1-z}\right)_+\right]\right.$$
$$\times\left[\frac{1}{2}(1+z^2)\left(1+\frac{1}{2}\frac{l^2}{Q^2}\right)+z^2\frac{x_1^2(l\cdot P_1)^{*2}+x_2^2(l\cdot P_2)^{*2}}{(Q^2)^2}\right.$$

$$+\frac{1}{2}\frac{1+z}{(1-z)_+}+\frac{1}{2}(1-z)\left(1+\frac{1}{2}\frac{l^2}{Q^2}\right)+\frac{(l\cdot P_1^*+l\cdot P_2^*)^2}{(Q^2)^2}\frac{z^2}{(1-z)_+}\Bigg\}$$
$$+\left(\frac{|\boldsymbol{l}|^3}{-l^2Q_0}\right)^*\frac{1}{(x_1+x_2)(1-z)}\left[\left(\frac{1}{y_+^*}+\frac{1}{(1-y^*)_+}\right)\right]\left[\left(1+\frac{1}{2}\frac{l^2}{Q^2}\right)\frac{1-z^2}{(1-z)_+}\right.$$
$$\left.+\frac{2z^2}{(1-z)_+}\frac{x_1^2(l\cdot P_1)^{*2}+x_2^2(l\cdot P_2)^{*2}}{(Q^2)^2}\right]-2\left(1+\frac{1}{2}\frac{l^2}{Q^2}\right)(1-z)\Bigg)\Bigg)+o(\varepsilon). \tag{71}$$

In Eq. (71), $P_{qq}(z)$ is defined [32] to mean

$$P_{qq}(z)=\frac{4}{3}\left[\frac{1+z^2}{(1-z)_+}+\frac{3}{2}\delta(1-z)\right] \tag{72}$$

and the asterisks are used [10] to indicate that the expression is evaluated at $y=y^*$. For later convenience, the independent variables have been changed from x_F and the three vector components of $\boldsymbol{l}$ to x_F, Q^2, and the previously defined angles θ_l and ϕ_l. The relations $l^2=4m_l^2-Q^2\simeq -Q^2$ and $l\cdot Q=0$ then imply that

$$\left.\begin{matrix}(l\cdot P_1)^*\\(l\cdot P_2)^*\end{matrix}\right\}=\frac{1}{2}\sqrt{s}\,\frac{\sqrt{-l^2}(|\mathbf{Q}|\cos\theta_{lQ}\pm Q_0\cos\theta_l)^*}{\sqrt{(Q_0^2-|\mathbf{Q}|^2\cos^2\theta_{lQ})^*}}, \tag{73a}$$

where

$$(|\mathbf{Q}|\cos\theta_{lQ})^*=\frac{1}{2}\sqrt{s}\left[x_F\cos\theta_l+\sin\theta_l\cos\phi_l\sqrt{\frac{\tau(1-z)}{z}\,y^*(1-y^*)}\right] \tag{73b}$$

$$\begin{aligned}(Q_0^2)^* &= Q^2+Q_3^2+Q_\perp^2\\ &= s[\tau+\tfrac{1}{4}x_F^2+\tau^{(1-z)^2/z}y^*(1-y^*)]\end{aligned} \tag{73c}$$

and the approximation of neglecting the lepton mass gives

$$1+\frac{1}{2}\frac{l^2}{Q^2}\sin^2\chi\simeq\frac{1}{2}(1+\cos^2\chi). \tag{73d}$$

Next the parton distributions are renormalized to order α_s (and all orders in leading logarithms). In the naive parton model the deep inelastic structure functions are given by

$$2F_1(x)=F_2(x)/x=\sum_q e_q^2[q(x)+\bar{q}(x)], \tag{74a}$$

where $q(x)$ and $\bar{q}(x)$ are the "bare" distributions of the various flavors of quark.

Beyond the leading order in QCD the parton densities are determined by the requirement that the form of Eq. (74) is preserved for the renormalized structure functions $F_2(x, t)$:

$$F_2(x, t) = \sum_q e_q^2 [q(x, t) + \bar{q}(x, t)], \tag{74b}$$

where $t = \ln(Q^2/\mu^2)$ and μ is an arbitrary scale of mass. This choice is made in order to conform to the conventions of Ref. [10].

The structure function $F_2(x, t)$ is calculated in perturbation theory in terms of the bare quark/parton distributions. To order α_s the resulting expression is then inverted to yield [10]

$$q(\bar{x}_1) = q(\bar{x}_1, t) - \alpha_s \int_{\bar{x}_1}^1 \frac{dx_1}{x_1} \left\{ \left[\frac{t}{2\pi} P_{qq}\left(\frac{\bar{x}_1}{x_1}\right) + f_{q,2}\left(\frac{\bar{x}_1}{x_1}\right) \right] q(x_1, t) + \left[\frac{t}{2\pi} P_{qG}\left(\frac{\bar{x}_1}{x_1}\right) + f_{G,2}\left(\frac{\bar{x}_1}{x_1}\right) \right] (G(x_2, t) \right\}, \tag{75a}$$

where $G(x_2, t)$ is the renormalized gluon distribution. The terms proportional to this gluon distribution are discussed later in the section on initial gluon diagrams and do not enter the present discussion. In Eq. (75), $f_{q,2}$ and $f_{G,2}$ are defined to order ε by the relations

$$f_{q,2}(z) = \frac{1}{2\pi}\frac{4}{3} \left\{ (1+z^2) \left(\frac{\ln(1-z)}{1-z} \right)_+ - \frac{3}{2} \frac{1}{(1-z)_+} - \frac{1+z^2}{1-z} \ln z + 3 + 2z - \left(\frac{9}{2} + \frac{\pi^2}{3} \right) \delta(1-z) - \frac{3}{4\varepsilon} P_{qq}(z) \right\} \left(\frac{4\pi\mu^2}{Q^2} \right)^{\varepsilon} \frac{1}{\Gamma(1-\varepsilon)} - \frac{\alpha_s}{2\pi} t P_{qq}(z) + o(\varepsilon) \tag{75b}$$

and

$$f_{G,2} = \frac{1}{2\pi} \cdot \frac{1}{2} \left\{ 2P_{qG}(z) \ln\left(\frac{1-z}{z} \right) + 6z(1-z) - \frac{2}{\varepsilon} P_{qG}(z) \right\} \left(\frac{4\pi\mu^2}{Q^2} \right)^{\varepsilon} \frac{1}{\Gamma(1-\varepsilon)} - \frac{\alpha_s}{2\pi} t P_{qG}(z) + o(\varepsilon) \tag{75c}$$

with [32]

$$P_{qG}(z) \equiv \tfrac{1}{2}[z^2 + (1-z)^2]. \tag{75d}$$

The function $\Delta q(x)$ is renormalized using a relation similar to Eqs. (75) but with q replaced by Δq. This simple substitution is valid because the radiation of a gluon by a

quark does not change the quark helicity, and therefore the difference $\Delta q = q^+ - q^-$ is preserved under renormalization.

The expression Eqs. (75) (without the terms proportional to $G(x_2, t)$) is substituted into the n-dimensional $q\bar{q}$ parton model cross section Eq. (69). All the order α_s $q\bar{q}$ annihilation contributions are summed. The remaining poles in ε cancel and the resulting cross section (written in terms of the *renormalized* distributions) is finite in the limit $\varepsilon \to 0$. The final result for the $\bar{q}$-polarized q contribution to the electromagnetic hadron–polarized hadron cross section is given by

$$\begin{aligned}
\underset{\text{integrated}}{d\sigma^{\text{EM}}(q\bar{q})} = {} & \frac{1}{2}\left(\frac{e_q}{e}\right)^2\left(\frac{e_l}{e}\right)^2\left(\frac{4}{9}\frac{\alpha_s}{2\pi}\right)\frac{\alpha^2}{s}\frac{dQ^2}{Q^2}\,d^2\Omega_l\,dx_F\,\frac{dx_1}{x_1}\frac{dx_2}{x_2} \\
& \times q(x_1, t)\,\bar{q}(x_2, t)\left(\left(1+\frac{1}{4}\frac{x_F^2}{\tau}\right)\left(1+\frac{1}{4}\frac{x_F^2}{\tau}\sin^2\theta_l\right)\right)^{-3/2} \\
& \times [\delta(x_1 z - x_2 + x_F) + \delta(x_2 z - x_1 - x_F)] \\
& \times \left(1+\frac{1}{2}\frac{l^2}{Q^2}\sin^2\chi\right)\left[\frac{1}{2}\left(1+\frac{4}{3}\pi^2\right)\delta(1-z) + 2\pi\cdot\frac{3}{4}\,g(z)\right] \\
& + \left(\frac{|l|^3}{-l^2 Q_0}\right)^* \frac{1}{(x_1+x_2)(1-z)}\left\{\left[\frac{1}{y_+^*} + \frac{1}{(1-y^*)_+}\right]\right. \\
& \times \left[\left(1+\frac{1}{2}\frac{l^2}{Q^2}\right)\frac{1+z^2}{(1-z)_+} + \frac{2z^2}{(1-z)_+}\frac{x_1^2(l\cdot P_1)^{*2} + x_2^2(l\cdot P_2)^{*2}}{(Q^2)^2}\right] \\
& \left.\left. - 2\left(1+\frac{1}{2}\frac{l^2}{Q^2}\right)(1-z)\right\}\right]. \qquad (76)
\end{aligned}$$

with [10]

$$\alpha_s\, g(z) \equiv \frac{\alpha_s}{2\pi}\cdot\frac{4}{3}\cdot\left[-2-3z+(1+z^2)\left(\frac{\ln(1-z)}{1-z}\right)_+ + \frac{3}{2}\frac{1}{(1-z)_+}\right]. \qquad (77)$$

(b) ELECTROWEAK CROSS SECTION. The charge-symmetric part of the electroweak interference contribution to the squared matrix element is proportional to the electromagnetic contribution in n dimensions. To complete the calculation of the electroweak interference contribution to the squared matrix element the *charge-antisymmetric* term are now calculated.

A definition of the traces involving the matrix γ_5 in n dimensions is required. The definition

$$\text{Tr}[\gamma_5 \boldsymbol{abed}] \equiv \frac{1}{4!}\varepsilon^{\mu\nu\rho\sigma}\,\text{Tr}[\gamma_\mu\gamma_\nu\gamma_\rho\gamma_\sigma \boldsymbol{abed}] \qquad (78)$$

(where $a \equiv a^{\mu}\gamma_{\mu}$) suffices [30]. The n-dimensional electroweak interference term for $q\bar{q}$ annihilation is found to be

$$2\,\mathrm{Re}[\bar{M}_{\mathrm{EM}} M_{\mathrm{weak}}]_{q\bar{q}} = g_s^2 e_q e_l [V_l(V_q - hA_q)\, S_\varepsilon(k', k'', Q, l) + A_l(A_q - hV_q)\, A_\varepsilon(k', k'', Q, l)], \tag{79a}$$

real gluon

where

$$A_\varepsilon(k', k'', Q, l) \equiv 32Q^2 \left[\frac{l\cdot k'}{k''^2} + \frac{l\cdot k''}{k'^2} - \frac{Q^2 l\cdot(k'+k'')}{k'^2 k''^2}\right] + 16\varepsilon \left[l\cdot k' \left(\frac{k''^2+Q^2}{k'^2} + \frac{k''-Q^2}{k''^2}\right) + l\cdot k'' \left(\frac{k'^2+Q^2}{k''^2} + \frac{k'^2-Q^2}{k'^2}\right)\right]. \tag{79b}$$

The dimensional regularization of the symmetric interference term $S_\varepsilon(k', k'', Q, l)$ was discussed in the previous section. The regularization of the charge-antisymmetric part of the interference term is similar. The variables y and z are substituted into $A_\varepsilon(k', k'', Q, l)$ which is then multiplied by the regulating phase space factors Eq. (63) and expanded as a power series in ε to yield

$$\begin{aligned}
&\frac{1}{32Q^2} z^{\varepsilon}(1-z)^{1-2\varepsilon}[y(1-y)]^{\varepsilon} A_\varepsilon(k', k'', Q, l) \\
&= -x_2 \frac{l\cdot P_2}{Q^2} z\left[-\frac{1}{\varepsilon}\delta(1-y) + \frac{1}{(1-y)_+} - \ln\left(\frac{z}{(1-z)^2}\right)\right] \\
&\quad + x_1 \frac{l\cdot P_1}{Q^2} z\left[-\frac{1}{\varepsilon}\delta(y) + \frac{1}{y_+} - \ln\left(\frac{z}{(1-z)^2}\right)\right] \\
&\quad - z^2 \frac{(x_1 l\cdot P_1 - x_2 l\cdot P_2)}{Q^2}\left[\frac{1}{2\varepsilon^2}\delta(1-z)[\delta(y)+\delta(1-y)]\right. \\
&\quad - \frac{1}{\varepsilon}\left\{\frac{1}{(1-z)_+}[\delta(y)+\delta(1-y)] + \frac{1}{2}\delta(1-z)\left[\frac{1}{y_+} + \frac{1}{(1-y)_+}\right]\right\} \\
&\quad + [\delta(y)+\delta(1-y)]\left\{-\frac{\ln z}{1-z} + 2\left[\frac{\ln(1-z)}{1-z}\right]_+\right\} \\
&\quad + \frac{1}{(1-z)_+}\left[\frac{1}{y_+} + \frac{1}{(1-y)_+}\right] \\
&\quad \left. + \frac{1}{2}\left\{\frac{\ln(1-y)}{y} + \frac{\ln y}{1-y} + \left(\frac{\ln y}{y}\right)_+ + \left[\frac{\ln(1-y)}{1-y}\right]_+\right\}\delta(1-z)\right)
\end{aligned}$$

$$+\frac{1}{2}\varepsilon\frac{(-x_2 l\cdot P_2)}{Q^2}\left[-\frac{1}{\varepsilon}\delta(y)+\frac{z}{\varepsilon}\delta(1-y)\right]$$

$$+\frac{1}{2}\varepsilon\frac{(x_1 l\cdot P_1)}{Q^2}\left[-\frac{1}{\varepsilon}\delta(1-y)+\frac{z}{\varepsilon}\delta(y)\right]+o(\varepsilon). \tag{80}$$

The charge-antisymmetric contribution to the cross section from the interference term Eq. (8) is then

$$\underset{\substack{\text{real}\\ \text{gluon}}}{d\sigma^{\text{EM}}(q\bar{q})} = \frac{e_l}{e}\frac{e_q}{e}\bar{q}(x_2)\,A_l[A_q q(x_1)-V_q\Delta q(x_1)]$$

$$\times\frac{\alpha}{2\pi}\cdot\frac{Q^2}{Q^2-M_Z^2}\left(\frac{4}{9}\frac{\alpha_s}{2\pi}(\mu^2)^{\varepsilon}\right)\frac{1}{Q^2 s}\left(\frac{|l|^3}{-l^2 Q_0}\right)$$

$$\times d^2\Omega_l\frac{dQ^2}{Q^2}\,dx_F\frac{dx_1}{x_1}\frac{dx_2}{x_2}\,dy\,\delta[(x_1+x_2)(1-z)y+x_1 z-x_2-x_F]$$

$$\times z^{\varepsilon}(1-z)^{1-2\varepsilon}[y(1-y)]^{-\varepsilon}\frac{1}{\Gamma(1-\varepsilon)}\cdot\frac{A_\varepsilon(k',k'',Q,l)}{32Q^2}. \tag{81}$$

The virtual gluon contribution to the charge-antisymmetric electroweak interference cross section is calculated by multiplying the parton model result

$$\underset{\text{parton}}{d\sigma^{\text{EW,c}}(q\bar{q})} = \frac{1}{3}\frac{e_q}{3}\frac{e_l}{e}A_l[A_q q(\bar{x}_1)_- - V_q\Delta q(\bar{x}_1)]\,\bar{q}(\bar{x}_2)$$

$$\times\frac{1}{8}\frac{\alpha}{2\pi}\left(\frac{-Q^2}{Q^2-M_Z^2}\right)\frac{1}{s}\frac{1+x_F^2/4\tau}{(1+x_F^2/4\tau\sin^2\theta_l)^{3/2}}\frac{dQ^2}{Q^2}\,d^2\Omega_l\,dx_F$$

$$\times\frac{dx_1}{x_1}\frac{dx_2}{x_2}\,\delta(1-z)\,\delta(x_1-x_2+x_F)\cos\chi \tag{82}$$

by the factor 2Γ defined in Eqs. (70).

The real and virtual gluon contributions to the charge-antisymmetric cross section are added, and, as in the pure electromagnetic case, the second-order poles in ε cancel. The remaining (first-order) poles in ε are absorbed into the scale-dependent quark/parton distributions as before. The final result is then finite in the limit $\varepsilon\to 0$. Thus the charge-antisymmetric $\bar{q}$-polarized q contribution to the integrated hadron–polarized hadron cross section is

$$\underset{\text{integrated}}{d\sigma^{\text{EW,c}}(q\bar{q})} = \frac{1}{3}\frac{e_q}{e}\frac{e_l}{e}\frac{A_l[q(x_1,t)\,A_q-\Delta q(x_1,t)\,V_q]}{4\pi}\bar{q}(x_2,t)$$

$$\times\left(\frac{-Q^2}{Q^2-M_Z^2}\right)\frac{\alpha}{s}\frac{dQ^2}{Q^2}\,d^2\Omega_l\,dx_F\frac{dx_1}{x_1}\frac{dx_2}{x_2}$$

$$
\times \left\{ \left\{ \left[1 + \left(\frac{4}{3} \frac{\alpha_s}{2\pi} \right) \left(1 + \frac{4}{3} \pi^2 \right) \right] \delta(1-z)\, \delta(x_2 - x_1 - x_F) + \left(\frac{4}{3} \frac{\alpha_s}{2\pi} \right) \right.
$$

$$
\times \left[\delta(x_2 z - x_1 - x_F) + \delta(x_1 z - x_2 + x_F) \right] \left[(1+z^2) \left(\frac{\ln(1-z)}{1-z} \right)_+ \right.
$$

$$
\left. + \frac{3}{2} \frac{1}{(1-z)_+} + \ln \left(\frac{z}{(1-z)^2} \right) - 3 - 2z \right] \Bigg\}
$$

$$
\times \cos\chi \frac{1 + x_F^2/4\tau}{(1 + x_F^2 \sin^2\theta_l/4\tau)^{3/2}}
$$

$$
+ \left(\frac{4}{3} \frac{\alpha_s}{2\pi} \right) \frac{2z}{(x_1 + x_2)(1-z)} \left(\frac{|l|^3}{-l^2 Q_0} \right)^*
$$

$$
\times \left\{ z \frac{x_1 l \cdot P_1^* - x_2 l \cdot P_2^*)}{Q^2} \left[\frac{1}{(1-z)_+} \left(\frac{1}{y_+^*} + \frac{1}{(1-y^*)_+} \right) \right] \right.
$$

$$
+ x_2 \frac{l \cdot P_2^*}{Q^2} \left[\frac{1}{y_+^*} - \ln \left(\frac{z}{(1-z)^2} \right) \right]
$$

$$
\left. + x_1 \frac{l \cdot P_1^*}{Q^2} \left[\frac{1}{(1-y^*)_+} + \ln \left(\frac{z}{(1-z)^2} \right) \right] \right\} + o(\alpha_s^2), \tag{83}
$$

where the squared lepton mass is neglected relative to Q^2.

By using counters which subtend large solid angles or by appropriate summation of the measured differential cross sections, it is possible to obtain an integrated asymmetry. The partially integrated charge, charge-helicity and helicity asymmetries are defined by

$$
a_c(Q^2, \Omega_l, x_F) \equiv \frac{\dfrac{d^4\sigma}{dQ^2\, d^2\Omega_l\, dx_F} - [\cos\theta_l \to -\cos\theta_l]}{\dfrac{d^4\sigma}{dQ^2 d^2\Omega_l dx_F} + [\cos\theta_l \to -\cos\theta_l]}, \tag{84a}
$$

$$
a_{\mathrm{ch}}(Q^2, \Omega_l, x_F) \equiv \frac{\dfrac{d^4\sigma_+}{dQ^2 d^2\Omega_l dx_F} + \dfrac{d^4\sigma_-}{dQ^2 d^2\Omega_l dx_F} - [\cos\theta_l \to -\cos\theta_l]}{\dfrac{d^4\sigma_+}{dQ^2 d^2\Omega_l dx_F} - \dfrac{d^4\sigma_-}{dQ^2 d^2\Omega_l dx_F} + [\cos\theta_l \to -\cos\theta_l]}, \tag{84b}
$$

$$
a_h(Q^2, \Omega_l, x_F) \equiv \frac{\dfrac{d^4\sigma_+}{dQ^2 d^2\Omega_l dx_F} - \dfrac{d^4\sigma_-}{dQ^2 d^2\Omega_l dx_F} + [\cos\theta_l \to -\cos\theta_l]}{\dfrac{d^4\sigma_+}{dQ^2 d^2\Omega_l dx_F} + \dfrac{d^4\sigma_-}{dQ^2 d^2\Omega_l dx_F} + [\cos\theta_l \to -\cos\theta_l]}. \tag{84c}
$$

These asymmetries are now calculated for πp collisions to first order in the weak interaction and Q^2/M_Z^2. The results are plotted for values of the strong coupling constant $\alpha_s = 0$ (parton model) and 0.2. The "running" of the coupling constant is neglected (as are scaling violations in the quark/parton distributions) because the effects of interest here do not depend strongly on these details. The quark/parton distributions are taken from Refs. [18] and [27], as previously.

The results for the asymmetrics are presented in the form (see Eqs. (39–(41)):

$$\left.\begin{matrix} a_c^{\pi^- p}(Q^2, \Omega_l, x_F) \\ a_c^{\pi^+ p}(Q^2, \Omega_l, x_F) \end{matrix}\right\} \simeq \frac{A_l}{(e_l/e)} \frac{1}{2\pi\alpha} \frac{Q^2}{M_Z^2} \left\{\begin{matrix} \dfrac{A_u}{(e_u/e)} H_c^{\pi^- p} \\ \dfrac{A_d}{(e_d/e)} H_c^{\pi^+ p} \end{matrix}\right.$$

$$\simeq 10^{-4} \frac{Q^2}{(\mathrm{GeV})^2} \begin{cases} -1.35 H_c^{\pi^- p} \\ -2.7 H_c^{\pi^+ p}, \end{cases} \tag{85}$$

where as usual $G_F = 1.17 \times 10^{-5}\ \mathrm{GeV}^{-2}$ and $\sin^2\theta_W = 0.225$. Similarly,

$$\left.\begin{matrix} a_{\mathrm{ch}}^{\pi^- p}(Q^2, \Omega_l, x_F) \\ a_{\mathrm{ch}}^{\pi^+ p}(Q^2, \Omega_l, x_F) \end{matrix}\right\} \simeq \frac{A_l}{(e_l/e)} \frac{1}{2\pi\alpha} \frac{Q^2}{M_Z^2} \left\{\begin{matrix} \dfrac{V_u}{(e_u/e)} H_{\mathrm{ch}}^{\pi^- p} \\ \dfrac{V_d}{(e_d/e)} H_{\mathrm{ch}}^{\pi^+ p} \end{matrix}\right.$$

$$\simeq 10^{-5} \frac{Q^2}{(\mathrm{GeV})^2} \begin{cases} 5.5 H_{\mathrm{ch}}^{\pi^- p} \\ 9.5 H_{\mathrm{ch}}^{\pi^+ p}, \end{cases} \tag{86}$$

$$\left.\begin{matrix} a_h^{\pi^- p}(Q^2, \Omega_l, x_F) \\ a_h^{\pi^+ p}(Q^2, \Omega_l, x_F) \end{matrix}\right\} \simeq \frac{V_l}{(e_l/e)} \frac{1}{2\pi\alpha} \frac{Q^2}{M_Z^2} \left\{\begin{matrix} \dfrac{A_u}{(e_u/e)} H_h^{\pi^- p} \\ \dfrac{A_d}{(e_d/e)} H_h^{\pi^+ p} \end{matrix}\right.$$

$$\simeq 10^{-5} \frac{Q^2}{(\mathrm{GeV})^2} \begin{cases} 1.4 H_h^{\pi^- p} \\ 2.8 H_h^{\pi^+ p}. \end{cases} \tag{87}$$

The quotient $H_c^{\pi p}$ is plotted versus $\cos\theta_l$ in Fig. 15, along with the corresponding lowest-order result. It is seen that the effect of the first-order perturbative QCD corrections is to increase the charge asymmetry by roughly 10%. The perturbative QCD corrections to the electroweak interference term and the pure electromagnetic cross section individually are much larger [10]—of the order of 60–80% in this case.

A similar result is seen in Fig. (16) for the quotient $H_{\mathrm{ch}}^{\pi p}$ corresponding to the π-polarized p charge-helicity asymmetry. Again, corrections to the asymmetry are

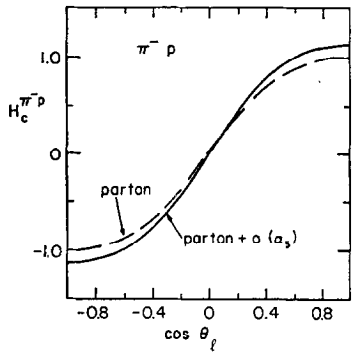

FIG. 15. The solid line is a plot of the quotient function $H_c^{\pi^- p}$ (the integrated charge asymmetry for $\pi^- p$ collisions) versus $\cos\theta_l$. The broken line depicts the corresponding parton model result (i.e., the integrated asymmetry with $\alpha_s = 0$). The other parameter values are $x_F = 0$, $\tau = 0.1$, $\cos\theta_l = 1$. The quotient function $H_c^{\pi^+ p}$ is extremely similar numerically.

small, while corrections to the electroweak numerator and electromagnetic denominator of this ratio are separately large.

The order α_s corrections to the helicity asymmetry are even smaller, as can be seen in Fig. 17. The remarkable numerical similarity between the parton model and parton model + $o(\alpha_s)$ results arises because the charge-symmetric portion of the electroweak interference matrix element is proportional to the squared electromagnetic matrix element (Eq. (79c)). Thus the large corrections to the respective cross sections occur in the same fashion in the numerator and denominator of the quotient function $H_h^{\pi p}$.

Note also the sign change in the asymmetry Fig. 17b as a function of τ, in accordance with the previous discussion of d quark polarization. This sign change also occurs for the charge-helicity asymmetry.

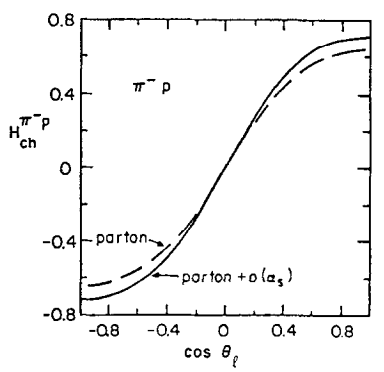

FIG. 16. The solid line is a plot of the quotient function $H_{ch}^{\pi^- p}$ (i.e. the integrated π^--polarized p charge-helicity asymmetry) versus $\cos\theta_l$, including both parton model and $o(\alpha_s)$ contributions. The broken line depicts the corresponding ratio calculated in the parton model. Unspecified parameters are as in Fig. 15.

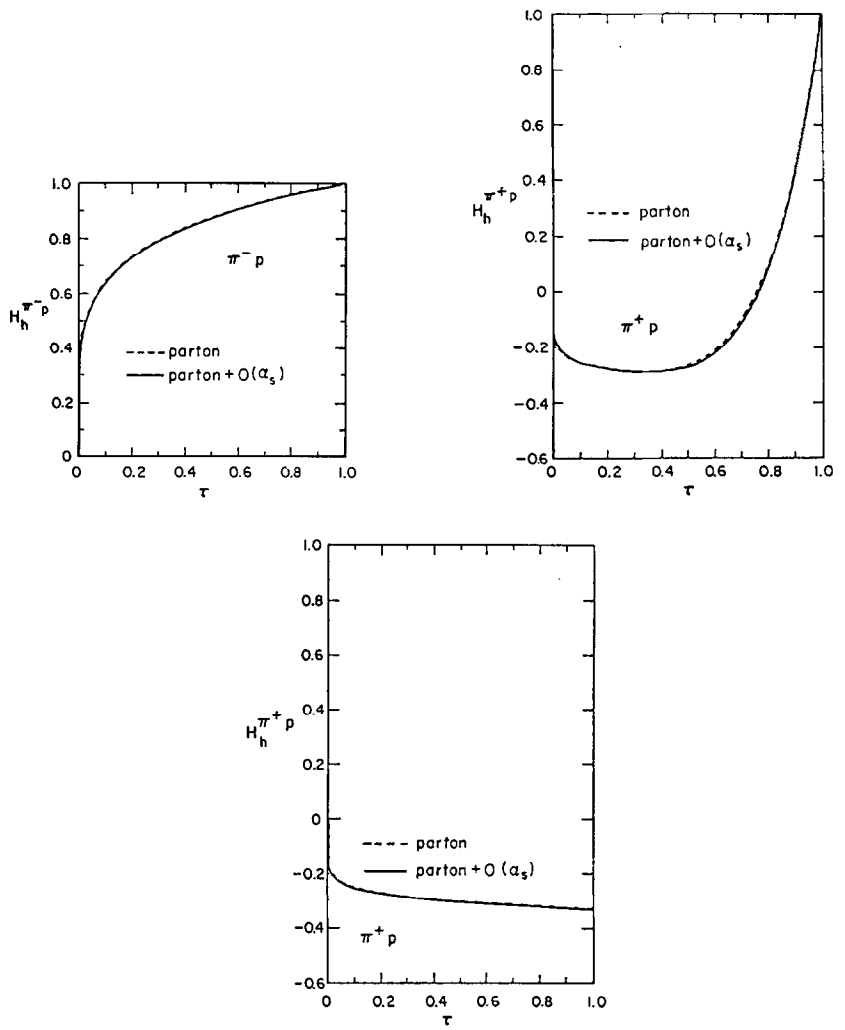

FIG. 17. (a) The solid line is a plot of the quotient function $H_h^{\pi^- p}$ (i.e., the integrated π^--polarized p helicity asymmetry) including parton model and $o(\alpha_s)$ contributions. The broken line depicts the corresponding ratio calculated in the parton model. Unspecified parameters are as in Fig. 15. (b) The solid line is a plot of the quotient function $H_h^{\pi^+ p}$ (the $\pi^+ p$ integrated helicity asymmetry) versus τ, calculated using the polarization function $\bar{\beta}_1(x)$. The broken line depicts the corresponding parton model result. Unspecified parameters are as in (a). (c) The same as (b), but for $\bar{\beta}_{11}(x)$.

3. *Initial gluon diagrams*

(a) ELECTROMAGNETIC CROSS SECTION. As pointed out previously, the kinematics of the initial gluon diagrams is different from that of quark–antiquark annihilation diagrams. The variables k' and k'' are redefined by Eq. (44), while the variables y and z are defined implicitly for the initial gluon graphs by

$$\text{initial gluon} \begin{cases} k'^2 \equiv \dfrac{Q^2}{z} = x_1 x_2 s, & \text{(88a)} \\ k''^2 \equiv \dfrac{-(1-z)}{z}(1-y)\,Q^2, & \text{(88b)} \\ (k''^2)^* = \dfrac{-x_2}{x_1+x_2}(x_1-\bar{x}_1)(x_1+\bar{x}_2)s, & \text{(88c)} \end{cases}$$

where to conform with the notation of Ref. [10] the asterisk implies evaluation at $y = y^*$. Kinematics requires that $k'^2 > Q^2$, as well as $x_1 > \bar{x}_1$, $x_2 > \bar{x}_2$. Equations (88) are substituted into the squared n-dimensional matrix element Eq. (56) and its overall sign is changed to account for the sign of the antiquark projection operator. The squared matrix element for the diagrams Figs. 2c and d is then seen to be

$$|M_{\mathrm{EM}}|^2_{qG} = e_q^2 e_l^2 g_s^2 S'_\varepsilon(k', k'', Q, l), \tag{89a}$$

where

$$\begin{aligned} &S'_\varepsilon(k', k'', Q, l) \\ &\quad = \frac{32Q^2z^2}{(1-z)(1-y)} \left\{ \left(1 - \varepsilon + \frac{1}{2}\frac{l^2}{Q^2}\right) \right. \\ &\qquad \times \left[\frac{z^2 + (1-z)^2 + 2z(1-z)(1-y) + (1-z)^2(1-y)^2}{2z^2} \right] \\ &\qquad + x_1^2 \frac{(l \cdot P_1)^2}{(Q^2)^2} + \frac{(x_1 l \cdot P_1 + x_2 l \cdot P_2)^2}{(Q^2)^2} \\ &\qquad \left. - \varepsilon \left(1 + \frac{1}{2}\frac{l^2}{Q^2}\right) \frac{[1-(1-z)(1-y)]^2}{2z^2} - \varepsilon x_2^2 \frac{(l \cdot P_2)^2}{(Q^2)^2} \right\} + o(\varepsilon^2). \end{aligned} \tag{89b}$$

The squared matrix element is regulated in much the same way as for the $q\bar{q}$ annihilation diagrams—the integration over $|\mathbf{Q}|$ is performed in n dimensions, while th outgoing quark momentum p' is eliminated via energy-momentum conservation. The phase space for the initial gluon graphs is therefore the same as for the annihilation graphs, Eq. (63).

Multiplication of the function $S'_\varepsilon(k', k'', Q, l)$ of Eq. (89) by the regulating phase space factors and expansion is a power series in ε yields

$$\begin{aligned} &\frac{1}{32Q^2} z^\varepsilon (1-z)^{1-2\varepsilon} [y(1-y)]^{-\varepsilon} S'_\varepsilon(k', k'', Q, l) \\ &\quad = -\frac{\delta(1-y)}{\varepsilon} P_{qG}(z) \left(1 + \frac{1}{2}\frac{l^2}{Q^2}\sin^2\chi\right) \end{aligned}$$

$$+\delta(1-y)\ln\left[\frac{(1-z)^2}{z}\right]P_{qG}(z)\left(1+\frac{1}{2}\frac{l^2}{Q^2}\sin^2\chi\right)$$

$$+\delta(1-y)\left[P_{qG}(z)+\frac{1}{2}\left(1+\frac{1}{2}\frac{l^2}{Q^2}\sin^2\chi\right)\right]$$

$$+\left(1+\frac{1}{2}\frac{l^2}{Q^2}\right)\left[P_{qG}(z)\frac{1}{(1-y)_+}+z(1-z)+\frac{1}{2}(1-z)^2(1-y)\right]$$

$$+\frac{1}{(1-y)_+}\left[x_1^2z^2\frac{(l\cdot P_1^*)^2}{(Q^2)^2}+z^2\frac{(x_1 l\cdot P_2^*+x_2 l\cdot P_1^*)^2}{(Q^2)^2}\right]. \tag{90}$$

Note that the most singular part is proportional to $1/\varepsilon$ (not $1/\varepsilon^2$) as there are no infrared singularities in initial gluon graphs.

The function $P_{qG}(z)$ is defined by [32]

$$P_{qG}(z)\equiv\tfrac{1}{2}[z^2+(1-z)^2]. \tag{91}$$

The initial gluon electromagnetic cross section, including $1/\varepsilon$ poles and scale invariant unrenormalized parton distributions is

$$\underset{\text{unrenormalized}}{d\sigma^{\text{EM}}(qG)} = \left(\frac{1}{6}\frac{\alpha_s}{2\pi}\right)\left(\frac{e_q}{e}\right)^2\left(\frac{e_l}{e}\right)^2\frac{\alpha^2}{s}\left(\frac{4\pi\mu^2}{Q^2}\right)^{\varepsilon}\frac{1}{\Gamma(1-\varepsilon)}$$

$$\times\frac{dQ^2}{Q^2}\,d^2\Omega_l\,dx_F\,\frac{dx_1}{x_1}\frac{dx_2}{x_2}\,q(x_1)\,G(x_2)\,\frac{(1+x_{F^2}/4\tau)}{(1+(x_F^2/4\tau)\sin^2\theta_l)^{3/2}}$$

$$\times\int dy\,\delta[(x_1+x_2)(1-z)y+x_1z-x_2-x_F]$$

$$\times z^{\varepsilon}(1-z)^{1-2\varepsilon}[y(1-y)]^{-\varepsilon}\frac{1}{32Q^2}\,S_{\varepsilon}'(k',k'',Q,l), \tag{92}$$

where the initial quark helicity is *not* averaged over.

The quark distributions are now renormalized to order α_s using the terms proportional to $G(x_1,t)$ in Eq. (75a) (which were previously ignored) but not including terms proportional to $q(x_1,t)$. This relation is inverted to give the quark distribution to order α_s:

$$q(x)=q(x,t)+\frac{1}{\varepsilon}\frac{1}{\Gamma(1-\varepsilon)}\frac{\alpha_s}{2\pi}\left(\frac{4\pi\mu^2}{Q^2}\right)^{\varepsilon}\int_0^1\frac{dy}{y}\theta(1-z)$$

$$\times\left\{P_{qG}(z)-\varepsilon\left[P_{qG}(z)\ln\left(\frac{1-z}{z}\right)+3z(1-z)\right]\right\}G(y,t), \tag{93}$$

where $z=x/y$. The expression Eq. (93) holds for Δq as well as for q. Equation (93) is substituted into the $q\bar{q}$ parton model expression for the electromagnetic cross section, Eq. (69). The order α_s contributions from both cross sections which involve the

functions $G(x, t)$ are summed. The $1/\varepsilon$ poles cancel, leaving a result which is finite as $\varepsilon \to 0$:

$$\begin{aligned}
\underset{\text{integrated}}{d\sigma^{\text{EM}}(qG)} = & \left(\frac{1}{6}\frac{\alpha_s}{2\pi}\right)\left(\frac{e_q}{e}\right)^2\left(\frac{e_l}{e}\right)^2 \frac{\alpha^2}{s}\frac{dQ^2}{Q^2}\, d^2\Omega_l\, dx_F \frac{dx_1}{x_1}\frac{dx_2}{x_2} \\
& \times q(x_1, t)\, G(x_2, t)\, \Bigg\{\delta(x_2 z - x_1 - x_F)\frac{1 + x_F^2/4\tau}{[1 + (x_F^2/4\tau)\sin^2\theta_l]^{3/2}} \\
& \times \left(1 + \frac{1}{2}\frac{l^2}{Q^2}\sin^2\chi\right)\left[P_{qG}(z)\ln(1-z) + \frac{1}{2} - 3z(1-z)\right] \\
& + \frac{1}{(x_1 + x_2)(1-z)}\left(\frac{|l|^3}{-l^2 Q_0}\right)^*\Bigg[\left(1 + \frac{1}{2}\frac{l^2}{Q^2}\right)P_{qG}(z)\frac{1}{(1-y^*)_+} \\
& + z(1-z) + \frac{1}{2}(1-z)^2(1-y^*) + \frac{1}{(1-y^*)_+}x_1^2 z^2 \frac{(l\cdot P_1)^{*2}}{(Q^2)^2} \\
& + \frac{z^2}{(1-y^*)_+}\frac{(x_1 l\cdot P_1^* + x_2 l\cdot P_2^*)^2}{(Q^2)^2}\Bigg]\Bigg\}. \qquad (94)
\end{aligned}$$

(b) ELECTROWEAK CROSS SECTION. As in the case of the electromagnetic cross section, the initial gluon variables Eqs. (88) are substituted into the n-dimensional electroweak contribution to the squared matrix element. This electroweak interference term is given by

$$\begin{aligned}
2\,\text{Re}[\bar{M}_{\text{EM}} M_{\text{W}}] = & g_s^2 e_q e_l [V_l(V_q - hA_q)\, S'_\varepsilon(k', k'', Q, l) \\
& + A_l(A_q - hV_q)\, A'_\varepsilon(k', k'', Q, l)], \qquad (95a)
\end{aligned}$$

where

$$\begin{aligned}
& \frac{1}{32Q^2} A'_\varepsilon(k', k'', l, Q) \\
& = -(x_1 l\cdot P_1 + x_2 l\cdot P_2)\frac{z}{(1-z)(1-y)} \\
& \quad + x_1 z l\cdot P_1 + (2x_1 l\cdot P_1 + x_2 l\cdot P_2)\frac{z^2}{(1-y)(1-y)} \\
& \quad + \frac{\varepsilon}{2}\left[(x_1 l\cdot P_1 + x_2 l\cdot P_2)\frac{z}{(1-z)(1-y)} - x_1 l\cdot P_1 \frac{1+z}{(1-z)(1-y)}\right). \qquad (95b)
\end{aligned}$$

Expression (95b) is multiplied by the regulating phase space Eq. (63) and expanded as a power series in ε to yield

$$\begin{aligned}
& \frac{1}{32Q^2}(1-z)^{1-2\varepsilon}[y(1-y)]^{-\varepsilon} A'_\varepsilon(k', k'', Q, l) \\
& \quad = -\frac{1}{\varepsilon}\cos\chi\, P_{qG}(z)\,\delta(1-y)
\end{aligned}$$

$$- \delta(1-y)\cos\chi \left\{ \frac{1}{4}(1+z^2) - P_{qG}(z) \ln\left[\frac{(1-z)^2}{z} \right] \right\}$$

$$- \frac{z}{(1-y)_+} [x_1(2z-1)\, l\cdot P_1 + x_2 + x_2(z-1) l\cdot P_2]$$

$$- x_1 z(1-z) l\cdot P_1 . \tag{96}$$

The corresponding contribution to the cross section is

$$\underset{\text{unrenormalized}}{d\sigma^{\mathrm{EW},c}(qG)} = \left(\frac{1}{6}\frac{\alpha_s}{2\pi}\right)\left(\frac{e_q}{e}\right)\left(\frac{e_l}{e}\right)\frac{1}{4\pi}\frac{\alpha}{s}\left(\frac{-Q^2}{Q^2-M_Z^2}\right)$$

$$\times A_l[q(x_1)\, A_q - \Delta q(x_1)\, V_q]\, G(x_2)\frac{|l|^3}{(-l^2)\, Q_0}$$

$$\times \frac{dQ^2}{Q^2} d^2\Omega_l\, dx_F \frac{dx_1}{x_1}\frac{dx_2}{x_2}\frac{1}{32Q^2} A'_6(k', k'', Q, l). \tag{97}$$

The parton distributions are now renormalized to order α_s (and all orders in leading logarithms). The order α_s charge-anitisymmetric initial gluon contribution to the cross section is then

$$\underset{\text{integrated}}{d\sigma^{\mathrm{EW},c}(qG)} = \left(\frac{1}{6}\frac{\alpha_s}{2\pi}\right)\left(\frac{e_q}{e}\right)\left(\frac{e_l}{e}\right)\frac{1}{4\pi}\frac{\alpha}{s}\left(\frac{-Q^2}{Q^2-M_Z^2}\right)$$

$$\times A_l[q(x_1,t)\, A_q - \Delta q(x_1,t)\, V_q]\, G(x_2,t)\frac{dQ^2}{Q^2} d^2\Omega_l\, dx_F \frac{dx_1}{x_1}\frac{dx_2}{x_2}$$

$$\times \left\{ \delta(x_2 z - x_1 - x_F)\cos\chi \frac{(1+x_F^2/4\tau)}{[1+(x_F^2/4\tau)\sin^2\theta_l]^{3/2}} \right.$$

$$\times \left[P_{qG}(z)\ln(1-z) + \frac{1}{4}(1+z^2) - 3z(1-z) \right]$$

$$+ \frac{z}{(1-y^*)_+}\left(\frac{|l|^3}{-l^2 Q_0}\right)^* [x_1(2z-1) l\cdot P_1^* + x_2(z-1) l\cdot P_2^*]$$

$$\left. + x_1 z(1-z)\left(\frac{|l|^3}{-l^2 Q_0}\right)^* l\cdot P_1^* \right\}, \tag{98}$$

where the asterisk denotes evaluation at $y = y^*$.

The various asymmetries are calculated to first order in the weak interaction and Q^2/M_Z^2 for proton–proton collisions. The cross sections for the $q\bar{q}$, qG and $\bar{q}G$ subprocesses are integrated over the longitudinal momentum fractions x_1 and x_2 and summed over quark flavors. The results for the various asymmetries are presented in the form

$$a_c^{pp}(Q^2, \Omega_l, x_F) = \frac{u}{(e_u/e)} \frac{A_l}{(e_l/e)} \frac{1}{2\pi\alpha} \frac{Q^2}{M_Z^2 H_c^{pp}}$$

$$\simeq -1.35 \times 10^{-4} \frac{Q^2}{(\mathrm{GeV})^2} H_c^{pp}, \tag{99a}$$

$$a_{\mathrm{ch}}^{pp}(Q^2, \Omega_l, x_F) = \frac{V_u}{(e_u/e)} \frac{A_l}{(e_l/e)} \frac{1}{2\pi\alpha} \frac{Q^2}{M_Z^2 H_{\mathrm{ch}}^{pp}}$$

$$\simeq 5.5 \times 10^{-5} \frac{Q^2}{(\mathrm{GeV})^2} H_{\mathrm{ch}}^{pp}, \tag{99b}$$

$$a_h^{pp}(Q^2, \Omega_l, x_F) = \frac{\mathrm{A}_u}{(e_u/e)} \frac{V_l}{(e_l/e)} \frac{1}{2\pi\alpha} \frac{Q^2}{M_Z^2} H_h^{pp}$$

$$\simeq 1.4 \times 10^{-5} \frac{Q^2}{(\mathrm{GeV})^2} H_h(pp), \tag{99c}$$

where as previously $\sin^2 \theta_W = 0.225$ is used for numerical values. The functions H^{pp} are calculated in the fashion of the functions Φ_{pp} defined previously. The denominator of each H^{pp} is given by

$$\frac{1}{e_u^2} \left[\sum_{q\bar{q}} \frac{d^4\sigma^{\mathrm{EM}}(q\bar{q})}{dQ^2 dx_F d^2\Omega_l} + \sum_q \frac{d^4\sigma^{\mathrm{EM}}(qG)}{dQ^2 dx_F d^2\Omega_l} + \sum_{\bar{q}} \frac{d^4\sigma^{\mathrm{EM}}(qG)}{dQ^2 dx_F d^2\Omega_l} \right] \tag{100}$$

while for example the numerator of H_c^{pp} is

$$\frac{1}{A_u e_u} \left[\sum_{q\bar{q}} \frac{d^4\sigma^{\mathrm{EW},c}(q\bar{q})}{dQ^2 dx_F d^2\Omega_l} + \sum_q \frac{d^4\sigma^{\mathrm{EW},c}(qG)}{dQ^2 dx_F d^2\Omega_l} + \sum_{\bar{q}} \frac{d^4\sigma^{\mathrm{EW},c}(\bar{q}G)}{dQ^2 dx_F d^2\Omega_l} \right]. \tag{101}$$

The notation $d\sigma^{\mathrm{EW},c}$ refers to that part of the electroweak interference cross sections which conserves parity and is antisymmetric under the exchange of the lepton pair four-momenta ("charge antisymmetric"). The definitions of the functions H_{ch}^{pp} and H_h^{pp} involve respectively the charge-antisymmetric and charge-symmetric parts of the analogous parity-*violating* electroweak cross section.

The integrated charge symmetry is plotted in Fig. 18 for $\alpha_s = 0.2$, $x_F = -0.5$, $\tau = 0.1$, and $\cos\phi_l = 1$. The parton model result (i.e., the $\alpha_s = 0$ integrated charge asymmetry) is also plotted, as well as the $q\bar{q}$ annihilation contribution to the asymmetry. The quark and antiquark parton distributions are taken from Ref. [18], while the gluon distribution is taken to be of the form Eq. (55) with $n = 7$ (to match the antiquark distribution[3]). Note that to first order in perturbative QCD the asymmetry

[3] A smaller value for n would allow the (negative) initial gluon contribution to dominate the parton model and order α_s annihilation contributions to the electromagnetic cross section as τ approaches one for fixed distributions and couplings. In this limit the cross section to this order thus becomes negative, reflecting inconsistencies in the parton distributions. This difficulty can be circumvented by using different scale dependent parton distributions and allowing the strong coupling constant to "run" with Q^2. Since the focus here is on the effects of a flavor $SU(2)$-asymmetric sea, the parton distributions of Ref. [18] suffice for this calculation.

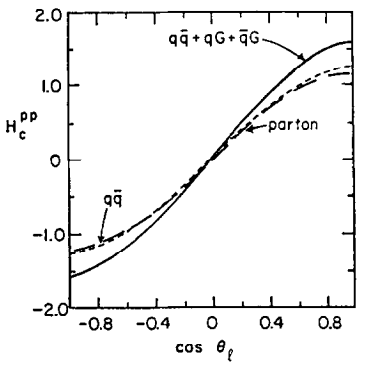

FIG. 18. The function H_c^{pp} (the integrated charge asymmetry for proton–proton collisions) is plotted versus $\cos\theta_l$ for the parameter values $\alpha_s = 0.2$, $x_F = -0.5$, $\tau = 0.1$, and $\cos\phi_l = 1$. The long-dash line shows the parton model (i.e., $\alpha_s = 0$) result, while the short-dash line shows the asymmetry resulting from the parton model and order α_s quark–antiquark annihilation contributions only.

arising from quark–antiquark annihilation alone is larger than the parton model result by roughly 10%. The corections to both the electroweak and electromagnetic cross section due to initial gluons are of opposite sign relative to the parton model result; the sum of all order α_s corrections gives an integrated charge asymmetry which is roughly 40% larger than the parton model value numerically.

Figure 19 displays the charge-helicity asymmetry as a function of $\cos\theta_l$ calculated using the parton distributions of Ref. [18], and a gluon distribution of the form Eq. (55) with $n = 7$. Note that to first order in perturbative QCD the asymmetry arising from quark–antiquark annihilation alone is larger than the parton mode.

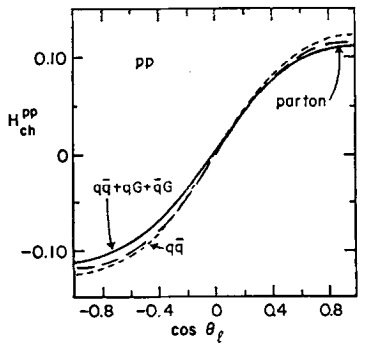

FIG. 19. The function H_{ch}^{pp} (the integrated charge-helicity asymmetry for proton–polarized proton collisions) is plotted versus $\cos\theta_l$ for the parameter values $\alpha_s = 0.2$, $x_F = 0$, $\tau = 0.1$, and $\cos\phi_l = 1$. The flavor $SU(2)$ asymmetry sea antiquark distributions of Ref. [18] are used, along with a gluon distributions of Ref. [18] are used, along with a gluon distribution of the form Eq. (55) with $n = 7$. The solid line displays the charge helicity asymmetry with all order α_s perturbative effects included. The short-dash line displays the asymmetry calculated using only the quark–antiquark annihilation contributions up to order α_s. The ling-dash line is the parton model result.

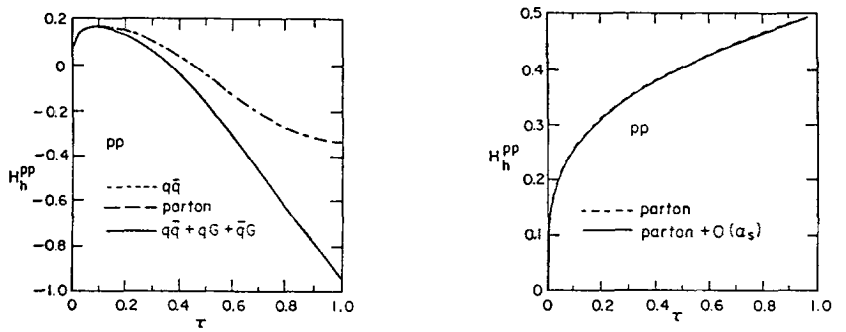

FIG. 20. (a) The function H_h^{pp} (the integrated helicity asymmetry for proton–polarized proton collisions) is plotted versus τ for the parameter values and distributions of Fig. 19, and $\cos\theta_l = 1$. The legend is also the same as in Fig. 19. (b) Same as (a) but with flavor $SU(2)$-symmetric sea antiquark distributions used (described in the text).

result by roughly 5%. The inclusion of the order α_s initial gluon corrections causes the total asymmetry to be reduced from the parton model result by roughly 5%.

The helicity asymmetry for proton–proton collisions is plotted in Fig. 20a using the parton distributions of Ref. [18] and the same gluon distribution as for Fig. 19. The sea quark distributions of Ref. [18] are flavor $SU(2)$-asymmetric—the $\bar{d}$ antiquark distribution is much larger than the $\bar{u}$ antiquark distribution for x near 1. This result for the asymmetry is contrasted with a similar calculation (Fig. 19b) performed with the use of $SU(2)$ symmetric distributions. These latter distributions are constructed by using the $\bar{d}$ antiquark distributions of Ref. [18] for both the $\bar{u}$ and $\bar{d}$ antiquark distributions.

As discussed previously, there is a sign change in the helicity asymmetry (as well as the charge-helicity asymmetry) as a function of τ for the flavor $SU(2)$-asymmetric sea. Note that the asymmetry calculated with the inclusion of initial gluon contributions exhibits a sign change at a value of $\tau \simeq 0.4$, which is less than the parton model value $\tau \simeq 0.5$.

IV. Off-Shell Quarks and Weak Asymmetries in Unpolarized Hadron-Hadron Collisions

A. *Quark–Antiquark Annihilation Diagrams*

In this section the possible occurence of parity violating effects in lepton pair production from *unpolarized* $q\bar{q}$ annihilation is considered. Should such an effect exist, it would produce a new parity-violating asymmetry in collisions of unpolarized hadrons proportional to

$$a^{PV} \sim \langle \mathbf{P} \cdot \boldsymbol{l}^+ \times \boldsymbol{l}^- \rangle. \tag{102}$$

Here $\mathbf{P}$ is the initial hadron momentum and l^+ and l^- are the lepton pair momenta. Such an asymmetry would be produced if a term proportional to

$$\varepsilon^{\mu\nu\rho\sigma} p_\mu p'_\nu l_\rho Q_\sigma \tag{103}$$

appeared in the $q\bar{q}$ cross section.

A term of this form does in fact occur in the electroweak $q\bar{q}$ cross section. It arises from the interference of the diagram Fig. 2a with the diagram Fig. 5b; this term is proportional to

$$\mathrm{Re}\left(\frac{1}{k'^2 - m_q^2 - i\varepsilon}\frac{1}{k''^2 - m_q^2 + i\varepsilon} i\varepsilon^{\mu\nu\rho\sigma} k'_\mu k''_\nu Q_\rho l_\sigma\right), \tag{104a}$$

where m_q^2 is the current quark mass. A term of this form also arises from the interference of the diagrams Figs. 2b and 5a; this term gives a contribution

$$-\mathrm{Re}\left(\frac{1}{k'^2 - m_q^2 - i\varepsilon}\frac{1}{k''^2 - m_q^2 - i\varepsilon} i\varepsilon^{\mu\nu\rho\sigma} k'_\mu k''_\nu Q_\rho l_\sigma\right). \tag{104b}$$

If both $k'^2 - m_q^2$ and $k''^2 - m_q^2$ are bounded away from zero the terms Eqs. (104) are each equal to zero. Even with an additional phase factor $e^{i\delta}$ (from, e.g., a vector meson resonance) introduced inside the parentheses in Eqs. (104) the sum of the two terms is still zero in this bounded kinematic region [12]. Therefore, in order for a parity-violating effect of this form to occur at this order of perturbative QCD, the kinematic variables cannot be so bounded. In fact, the sum of the two terms Eq. (104) is proportional to

$$\left[\frac{\delta(k'^2 - m_q^2)}{k''^2 - m_q^2} - \frac{\delta(k''^2 - m_q^2)}{k'^2 - m_q^2}\right] \varepsilon^{\mu\nu\sigma\rho} k'_\mu k''_\nu Q_\sigma l_\rho. \tag{105}$$

Consider how such a term might contribute. Suppose the incoming quarks and outgoing gluon in the diagrams Figs. 2a and b and 5a and b are massless and on their mass shell. Then if k'^2 or k''^2 is equal to zero (in order to satisfy the delta functions in Eq. (105)) only two of the momentum four-vectors k'_μ, k''_μ, and Q_μ are linearly independent, and the antisymmetric ε symbol in Eq. (105) vanishes. It follows that to this order in perturbative QCD off-mass-shell (or massive) quarks are required for a nonvanishing asymmetry [19].

For any calculation of such an asymmetry explicit assumptions about quark binding effects and/or masses must therefore be made. Such assumptions are outside the domain of the usual perturbative QCD treatment, where initial quarks are taken to be on mass shell with zero current mass. These assumptions are not justified if the poles of quark propagators are absorbed *completely* by the confinement mechanism. However the use of perturbative QCD appears to be satisfactory even in the presence of on-shell intermediate-state quarks as no explicit singularities (logarithmic divergences) occur.

As the current quark masses for light quarks are likely to be extremely small relative to all other momentum scales in the problem, they should produce only very small effects. Thus the possible effects of off-mass–shell quarks are considered here, and m_q is set equal to zero.

Consider the kinematics of diagram Fig. 2a. For a nonzero asymmetry either k'^2 or k''^2 must be zero; thus look at the case $k'^2 = 0$. From the definition of k' for $q\bar{q}$ annihilation, Eq. (4c), it follows that

$$p^2 = k'^2 + k^2 + 2k \cdot k' = 2k_0 k_0' \left(1 - \frac{k_0'}{|k_0'|} \cos \theta_{kk'}\right) \tag{106}$$

as both k'^2 and k^2 are equal to zero. The strict inequalities $-1 < \cos \theta_{kk'} < 1$ must hold in order that four independent momenta remain (so the term Eq. (103) is nonzero). Since the energy of a final state gluon is positive ($k_0 > 0$), p^2 is of the same sign as k_0'. It is easy to see that

$$p'^2 = Q^2 - |p' \cdot Q| \operatorname{sign}(k_0'). \tag{107}$$

Thus if $p^2 < 0$ (i.e., if p^2 is spacelike), p'^2 must be greater than Q^2 in order to obtain a nonvanishing asymmetry. This is unlikely to occur at sufficiently large values of Q^2 ($\lesssim 100\,\mathrm{GeV}^2$) for which weak asymmetries are large enough ($\gtrsim 10^{-4}$) to be measurable. Thus the initial quark and antiquark must be *timelike* to get an observable (and measurable!) effect to this order in perturbative QCD.

The assumption of the existence of timelike quarks [19] inside a hadron sets a different course than is usually followed. In the off-mass-shell procedure for the regularization of massless QCD [10, 11, 33], for example, the initial quarks are assumed to be off shell in the *spacelike* direction from binding effects so as to remove the collinear singularities from the physical region. However, if asymmetries of the form Eq. (105) are actually observed experimentally (and in particular if the measured asymmetry is large) it will be difficult to reconcile with the usual treatment of perturbative QCD. The order of magnitude of such effects is estimated next, assuming the usual ($\sim$1 GeV) scale of binding effects.

In order to have an *effective* description of the nonperturbative effects of quark binding, "mass" and transverse momentum distribution functions for the incoming quarks in the incident hadrons are introduced. The various momenta are defined by

$$\begin{aligned} \mathbf{p} &= -x_1 P_0 \hat{z} + \mathbf{p}_\perp, & \mathbf{p}' &= x_2 P_0 \hat{z} + \mathbf{p}_\perp', \\ p_0 &= (p^2 + \mathbf{p}^2)^{1/2}, & p_0' &= (p'^2 + \mathbf{p}'^2)^{1/2}. \end{aligned} \tag{108}$$

The full distribution for the initial antiquarks and quarks in the incident hadrons are taken to be

$$\begin{aligned} dN_{\bar{q}} = {} & (\pi\sigma^2\sigma_\perp^2)^{-1}\, dp'^2\, d^2\mathbf{p}_\perp'\, dx_2 \\ & \times \exp(-p'^2/\sigma^2) \exp(-\mathbf{p}_\perp'^2/\sigma_\perp^2)\, \bar{q}(x_2), \end{aligned} \tag{109a}$$

$$dN_q = (\pi\sigma^2\sigma_\perp^2)^{-1}\, dp^2\, d^2\mathbf{p}_\perp\, dx_1$$
$$\times \exp(-p^2/\sigma^2)\exp(-\mathbf{p}_\perp^2/\sigma_\perp^2)\, q(x_1) \qquad (p^2, p'^2 > 0). \tag{109b}$$

The $q\bar{q}$ contribution to the hadronic cross section is then

$$d\sigma_{\text{hadron}} = \int dN_q\, dN_{\bar{q}}\, d\sigma(q\bar{q}), \tag{110}$$

where $d\sigma(q\bar{q})$ is the differential quark cross section. The parity-violating quark cross section arising from the interference of the diagram Fig. 2a with the diagram Fig. 5b and the diagram Fig. 2b with the diagram Fig. 5a is [19] (in the c.m. frame):

$$d\sigma^{PV}(qq) = \left(\frac{4}{9}\frac{\alpha_s}{2\pi}\right)\frac{\alpha}{M_Z^2 Q^2}\left(\frac{e_q}{e}\right)\left(\frac{e_l}{e}\right)\frac{2}{\pi^2}$$
$$\times \frac{1}{p_0}\cdot\frac{1}{p_0'}\frac{d^3l^+\, d^3l^-}{l_0^+ l_0^-}\varepsilon^{\mu\nu\omega\rho} p_\mu\, p'_\nu\, l_\omega\, Q_\rho$$
$$\times \left\{V_l A_q\, l\cdot(p'-p) + \frac{1}{2}V_q A_l[(p-p')^2 - Q^2]\right\}$$
$$\times \theta(k_0)\,\delta(k^2)\left[\frac{\delta(k'^2)}{k''^2} - \frac{\delta(k''^2)}{k'^2}\right] \tag{111}$$

(where $k_\mu = p_\mu + p'_\mu - Q_\mu$) which includes the color factor 4/9. The weak coupling constants are defined in Eqs. (2); since experimentally $\sin^2\theta_W \approx \frac{1}{4}$, the term involving $V_l \sim (1 - 4\sin^2\theta_W)$ is small and can be neglected. In addition, the assumptions $\sigma_\perp^2 = \sigma^2$ and $Q^2 \gg \sigma^2$ (i.e. $x_1, x_2 \gg \sigma/p_0$ over their range of integration) are used.

First consider the term in Eq. (111) proportional to $\delta(k'^2)$. Define the new variables

$$\eta^2 \equiv p^2 + 2\mathbf{k}'_1\cdot\mathbf{p}_\perp, \tag{112a}$$

$$x_1^* \equiv -\frac{\eta^2}{\sqrt{s}\,\mathbf{k}'^2_\perp \bar{x}_1}\left[|k'_3| - k'_0\frac{\sqrt{1 - 4\mathbf{k}'^2_\perp(p^2 + \mathbf{p}_\perp^2)}}{(\eta^2)^2}\right] \tag{112b}$$

and expand to first order in $\sigma^2/(x_1 P_0)^2$ to find

$$Q^2 \simeq (p-p')^2 \simeq Q^2(1 + x_1^*), \tag{113a}$$

$$\theta(k_0) \simeq \theta(x_1^* - 1), \tag{113b}$$

$$\frac{1}{p_0}\delta(k^2) \simeq \frac{\delta(x_1 - \bar{x}_1 x_1^*)}{P_0\sqrt{(\eta^2)^2 - 4\mathbf{k}'^2_\perp(p^2 + p_\perp^2)}}, \tag{113c}$$

$$(Q-p)^2 \simeq Q^2(1-x_1^*), \tag{113d}$$

$$\frac{1}{p_0'}\,\delta(k'^2) \simeq \frac{\delta(x_2-\bar{x}_2)}{P_0 Q^2}. \tag{113e}$$

Note the simplifications that result taking the combinations in Eqs. (113).

The delta functions in $d\sigma^{PV}(q\bar{q})$ imply the existence of a threshold value in p^2 for the $\delta(k'^2)$ term (and a corresponding threshold in p'^2 for the term proportional to $\delta(k''^2)$). Since the integrand in $d\sigma^{PV}(q\bar{q})$ has a square-root divergence when p^2 (or p'^2) is at this threshold value, the integral over $p^2(p'^2)$ can be approximated by factoring out this singularity and evaluating the rest of the integrand at its threshold value. The singular part of the integrand is then integrated over $p^2(p'^2)$. This procedure yields the result:

$$(\eta^2)^2 - 4\mathbf{k}''^2_\perp(p^2+\mathbf{p}_\perp^2) \simeq (p^2+\bar{p}^2)(p^2-p_{\text{th}}^2), \tag{114a}$$

$$p^2+\bar{p}^2 \simeq p_{\text{th}}^2+\bar{p}^2 = 4\,|\mathbf{k}_\perp|\,|\mathbf{k}'_\perp|, \tag{114b}$$

$$\begin{aligned}\int_{p_{\text{th}}^2}^{\infty}\frac{dp^2}{\sigma^2}\,\frac{e^{-p^2/\sigma^2}}{\sqrt{(\eta^2-4\mathbf{k}'^2_\perp(p^2+\mathbf{p}_\perp^2)}} &\simeq \frac{1}{2}\,(|\mathbf{k}_\perp|\,|\mathbf{k}'_\perp|)^{-1/2}\int_{p_{\text{th}}^2}^{\infty}\frac{dp^2}{\sigma^2}\,\frac{e^{-p^2/\sigma^2}}{\sqrt{p^2-p_{\text{th}}^2}} \\ &= \frac{1}{2}\,(|\mathbf{k}_\perp|\,|_{\mathrm{k}\perp}'|)^{-1/2}\,\frac{\sqrt{\pi}}{\sigma}\,e^{-p_{\text{th}}^2/\sigma^2}\end{aligned} \tag{114c}$$

and the remaining factors in this contribution to the cross section are evaluated at $p^2 = p_{\text{th}}^2$. Here, p_{th}^2 is given by

$$p_{\text{th}}^2 = 2(|\mathbf{k}_\perp|\,|\mathbf{k}'_\perp| - \mathbf{k}_\perp\mathbf{k}'_\perp). \tag{115}$$

In particular, the angular averaged pseudoscalar becomes

$$\langle \varepsilon^{\mu\nu\omega\rho} p'_\mu p_\nu l_\omega Q_\rho\rangle = \tfrac{1}{2}Q^2(x_1^*-1)\,\hat{Q}_\perp \times \boldsymbol{l}_\perp \cdot \hat{z}\,|\mathbf{k}'_\perp| \tag{116}$$

plus terms which vanish upon the angular integration in $\mathbf{p}_\perp$ and $p'_\perp$. The contribution of the $\delta(k'^2)$ term to the parity-violating hadronic cross section can be expressed to first order in Q^2/M_Z^2 as

$$\begin{aligned}d_{\text{hadron}}^{PV} = &\frac{d^2k_\perp}{\pi\sigma^2}\,\frac{d^2k'}{\pi\sigma^2}\,\frac{1}{\pi}\left(\frac{e_q}{e}\right)\left(\frac{e_l}{e}\right)\left(\frac{4}{9}\,\frac{\alpha_s}{2\pi}\right)\frac{\alpha}{Q^2 s}\,\frac{A_l V_q}{M_Z^2}\,\frac{d^3l^+ d^3l^-}{l_0^+ l_0^-} \\ &\times (\boldsymbol{l}_\perp \times \mathbf{k}'_\perp \cdot \hat{z})(1+x_{\text{th}}^*)\,\delta(x_2-\bar{x}_2)\,\delta(x_1-\bar{x}_1 x_{\text{th}}^*)\,\theta(x_{\text{th}}^*-1) \\ &\times (|\mathbf{k}_\perp|\,|\mathbf{k}'_\perp|)^{-1/2}\,\frac{\pi^{1/2}}{\sigma}\,e^{[(\mathbf{k}'_\perp-\mathbf{Q}_\perp)^2+(|\mathbf{k}'_\perp|+|\mathbf{k}_\perp|)^2]/\sigma^2},\end{aligned} \tag{117a}$$

where

$$x_{1,\text{th}}^* \simeq 1+\frac{|\mathbf{k}_\perp|}{|\mathbf{k}'_\perp|}. \tag{117b}$$

The x_1 delta function is now used to perform the $|\mathbf{k}_\perp|$ integration, while the angular $d\Omega_{k_\perp}$ integration contributes a factor 2π since the integrand is independent of the angle of $\mathbf{k}_\perp$. Upon performing the $\boldsymbol{k}_\perp$ and the $\mathbf{k}'_\perp$ integrations, the parity-violating hadronic cross section is found to be

$$\begin{aligned} d\bar{\sigma}^{PV}_{\text{hadron}} \cong & -\frac{1}{6}\left(\frac{e_q}{e}\right)\left(\frac{e_l}{e}\right)\left(\frac{4}{3}\frac{\alpha_s}{2\pi}\right)\frac{\alpha}{Q^2 s}\frac{A_l V_q}{M_Z^2}\frac{d^3l^+ d^3l^-}{l_0^+ l_0^-}\,dx_1\,dx_2 \\ & \times e^{-\mathbf{Q}_\perp^2/\alpha^2}\left(\frac{|\mathbf{Q}_\perp|}{\sigma}\right)\left(\frac{|\boldsymbol{l}_\perp|}{\sigma}\right)(\hat{z}\cdot\hat{Q}_\perp\times\hat{l}_\perp)\,q(x_1)\,\bar{q}(x_2) \\ & \times\{\delta(x_2-\bar{x}_2)\,\theta(x_1-\bar{x}_1)(x_1+\bar{x}_1)(x_1-\bar{x}_1)^{1/2}(x_1^2+\bar{x}_1^2)^{-5/2} \\ & \times \bar{x}_1^{5/2}e^{r_1}[(3+4r_1)\,I_0(r_1)+(1+4r_1)\,I_1(r_1)]\}-[1\leftrightarrow 2]. \end{aligned} \tag{118a}$$

Here r_n is defined by

$$r_n \equiv \frac{1}{2}\frac{|\mathbf{Q}_\perp|^2}{\sigma^2}\left(1+\frac{x_n^2}{\bar{x}_n^2}\right)^{-1} \tag{118b}$$

and I_n is the modified nth-order Bessel function [35]. The result Eq. (118) is antisymmetrized in the indices 1 and 2 in order to include the contributions of both propagator terms.

To calculate the parity-violating asymmetry, the ratio of the parity-violating cross section to the parity-conserving cross section is needed. To lowest order in the strong coupling constant α_s, the parity-conserving quark cross section is given by the simple Drell–Yan formula Eq. (3a). When the transverse momentum and "mass" distributions Eqs. (109) are applied in the fashion of Eq. (110), the parity-conserving hadronic cross section is found to be [19]:

$$d\sigma^{\text{DY}}_{\text{hadron}} \simeq \frac{1}{3}\left(\frac{e_q}{e}\right)^2\left(\frac{e_l}{e}\right)^2\frac{\alpha^2}{Q^2 s}\frac{d^3l^+ d^3l^-}{l_0^+ l_0^-}\frac{e^{-|\mathbf{Q}_\perp|^2/2\sigma^2}}{\pi\sigma^2}\,q(\bar{x}_1)\,\bar{q}(\bar{x}_2), \tag{119}$$

where a sum over flavors is understood. The result Eq. (119) is valid in a kinematic region where $l\cdot p$ and $l\cdot p'$ are both small compared to Q^2 (i.e., $\boldsymbol{l}_\perp$ is the largest component of $\boldsymbol{l}$). The asymmetry is maximized in this kinematic region, and is given explicitly for πp collisions by

$$a^{PV} \equiv \frac{d^6\sigma^{PV}_{\text{hadron}}/d^3l^+\,d^3l^-}{d^6\sigma^{DY}_{\text{hadron}}/d^3l^+\,d^3l^-} \tag{120a}$$

$$\left.\begin{matrix} a^{PV}(\pi^- p) \\ a^{PV}(\pi^+ p) \end{matrix}\right\} \simeq \frac{-\alpha_s}{\alpha}(\hat{z}\cdot\hat{Q}_\perp\times\hat{l}_\perp)\frac{\sigma|\boldsymbol{l}_\perp|}{64M_Z^2}\frac{A_l}{(e_l/e)} \times \begin{cases} \dfrac{V_u}{(e_u/e)}\,[L_1(u_p)-L_2(\bar{u}_\pi)] \\ \dfrac{V_d}{(e_d/e)}\,[L_1(d_p)-L_2(\bar{d}_\pi)], \end{cases} \tag{120b}$$

$$\simeq \hat{z}\cdot\hat{Q}_\perp \times \hat{l}_\perp \begin{cases} -5.4\times 10^{-6}[L_1(u_p)-L_2(\bar{u}_\pi)] \\ -9.3\times 10^{-6}[L_1(d_p)-L_2(\bar{d}_\pi)] \end{cases} \tag{120c}$$

for $|\mathbf{Q}_\perp| = 2\sigma = 1$ GeV, $|\boldsymbol{l}_\perp| \simeq 10$ GeV, $\alpha_s \simeq 0.2$, and $\sin^2\theta_W \simeq 0.225$. Note that kinematics requires $|\boldsymbol{l}_\perp|^2 \gtrsim Q^2$ if $\boldsymbol{l} \simeq \boldsymbol{l}_\perp$. The functional $L_n(q)$ is given by

$$L_n(q) \equiv 8\,\frac{\exp(-|\mathbf{Q}_\perp|^2/2\sigma^2)}{q(\bar{x}_n)}\,\frac{|\mathbf{Q}_\perp|}{\sigma}\,\bar{x}_n^{5/2}$$
$$\times \int_{\bar{x}_n}^{1} dx_n (x_n+\bar{x}_n)(x_n-\bar{x}_n)^{1/2}(x_n^2+\bar{x}_n^2)^{-5/2} q(x_n)$$
$$\times [(3+4r_n)I_0(r_n)+(1+4r_n)I_1(r_n)]\,e^{r_n}. \tag{120d}$$

The difference $L_1 - L_2$ is plotted in Fig. 21. Note that the asymmetry is maximum when $|\mathbf{Q}_\perp| \approx 2\sigma$, $\tau = 0.25$ and when x_F is large. Thus Q has an appreciable longitudinal component.

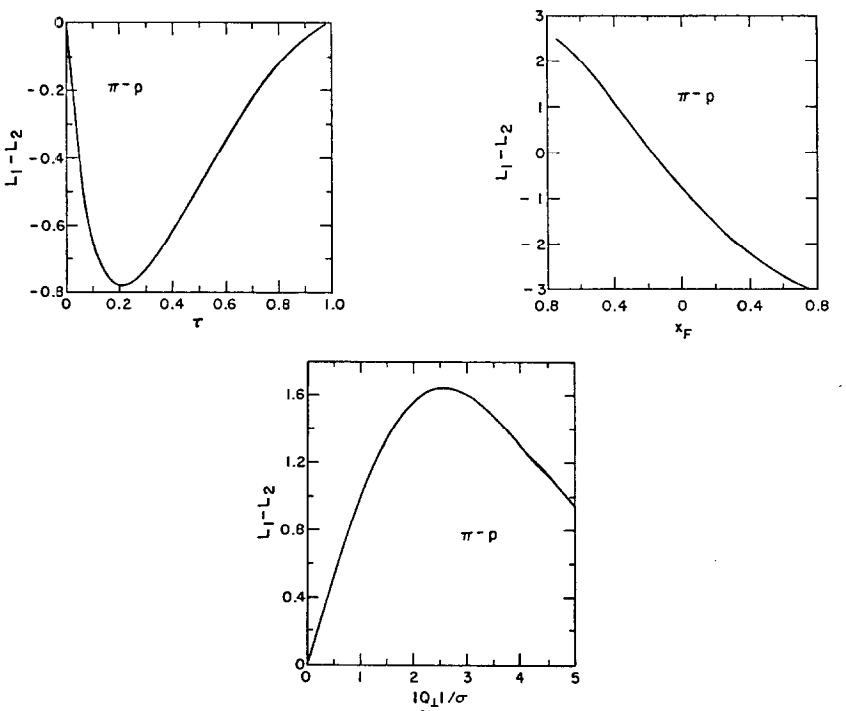

FIG. 21. (a) The difference $L_1(u_p) - L_2(\bar{u}_\pi)$ (i.e. the parity-violating asymmetry for π^--*unpolarized* p collisions) is plotted versus τ. The other parameters are $|\mathbf{Q}_\perp|/\sigma = 2$, $x_F = 0$. The proton and pion distributions are taken from Refs. [18] and [27]. (b) The difference $L_1(u_p) - L_2(\bar{u}_\pi)$ of (a) plotted versus x_F. The other parameter values are $|\mathbf{Q}_\perp|/\sigma = 2$, $\tau = 0.25$. (c) The difference $L_1(u_p) - L_2(\bar{u}_\pi)$ of (a) plotted versus $|\mathbf{Q}_\perp|/\sigma$. The other parameter values are $\tau = 0.25$ and $x_F = 0.5$.

The order of magnitude of this result may be understood simply by considering the essential factors in Eq. (120b),

$$\frac{a^{PV}}{L_1 - L_2} \simeq \frac{\alpha_s}{\alpha} \frac{G_F |\boldsymbol{l}_\perp| \sigma}{64} \hat{z} \times \hat{Q}_\perp \cdot \hat{l}_\perp$$
$$\simeq 10^{-5} \hat{z} \times \hat{Q}_\perp \cdot \hat{l}_\perp \qquad \text{for} \quad Q^2 \simeq 100\ \text{GeV}^2. \tag{121}$$

B. *Initial Gluon Diagrams*

For πp collisions, initial gluon diagrams are relatively unimportant numerically. However, they are of crucial importane for pp collisions. Therefore the analysis of the previous section is now applied to the initial gluon diagrams Figs 2c and d and 5c and d.

An important feature of the initial gluon diagrams is that kinematics requires $k'^2 \geqslant Q^2$ for massless quarks, and so only the second term in Eq. (105) can contribute to the parity violation. The kinematics of the contributing initial gluon term is very similar to the kinematics of the annihilation graphs. The existence of a nonzero asymmetry arising via the initial gluon diagrams requires the initial gluon to be timelike. Therefore, gluon "mass" and transverse momentum distributions are introduced. The kinematic variables of the initial quark and gluon are defined by

$$\begin{aligned} \mathbf{p} &= -x_1 P_0 \hat{z} + \mathbf{p}_\perp, \qquad & p_0 &= (p^2 + \mathbf{p}^2)^{1/2}, \\ \mathbf{k} &= x_2 P_0 \hat{z} + \mathbf{k}_\perp, \qquad & k_0 &(k^2 + \mathbf{k}^2)^{1/2}. \end{aligned} \tag{122}$$

The full distribution function for the initial quark is given by Eq. (109b); that for the gluon is

$$dN_G = (\pi\sigma^2\sigma_\perp^2)^{-1}\, dk^2\, d^2\mathbf{k}_\perp\, dx_2$$
$$\times \exp(-k^2/\sigma^2) \exp(-\mathbf{k}_\perp^2/\sigma_\perp^2)\, G(x_2). \tag{123}$$

The contribution to the lepton pair production cross section from quark–gluon scattering is then given by

$$d\sigma_{\text{hadron}} = \int dN_q\, dN_G\, d\sigma(qG), \tag{124}$$

where the sum over flavor is understood and $d\sigma(qG)$ represents the appropriate initial gluon cross section. The parity-violating initial gluon contribution to the cross section is (compare Eq. (111)):

$$d\sigma^{PV}(qG) = \left(\frac{1}{6}\frac{\alpha_s}{2\pi}\right)\frac{\alpha}{M_Z^2 Q^2}\left(\frac{e_q}{e}\right)\left(\frac{e_l}{e}\right)\frac{2}{\pi^2}$$
$$\times \frac{1}{k_0}\frac{1}{p_0}\frac{d^3l^+ d^3l^-}{l_0^+ l_0^-}\varepsilon^{\mu\nu\omega\rho} k_\mu p_\nu l_\omega Q_\rho$$
$$\times \{V_l A_q\, l \cdot (2p + k) + \tfrac{1}{2} V_q A_l [Q^2 - (2p + k - Q)^2 + k^2]\}$$
$$\times \theta(p_0')\, \delta(p'^2) \left[\frac{-\delta(p - Q)^2}{2p \cdot k}\right] \tag{125}$$

with $p'_\mu = p_\mu + k_\mu - Q_\mu$ by the conservation of four-momentum. This expression holds in the quark–gluon c.m. frame

The calculation of the quark–gluon scattering contribution to the parity-violating hadronic cross section is straightforward and follows closely the analysis presented for the $q\bar{q}$ annihilation graphs. For example, the relations corresponding to Eqs. (112) are

$$\xi^2 \equiv -k^2 + 2\mathbf{k}''_\perp \cdot k, \tag{126a}$$

$$x_2^* \equiv \frac{\xi^2}{\sqrt{s}\,\mathbf{k}''^2_\perp \bar{x}_2}\left[|k''_3| - k''_0\sqrt{\frac{1 - 4\mathbf{k}''^2_\perp(k^2 + \mathbf{k}^2_\perp)}{\xi^4}}\right]. \tag{126b}$$

The quark–gluon scattering contribution possesses a square-root divergence of the same form as the annihilation cross section (compare Eq. (113c)):

$$\frac{\delta(p'^2)}{k_0} = \frac{\delta(x_2 - x_2^*\bar{x}_2)}{P_0\xi^2\sqrt{1 - 4k''^2_\perp(k^2 + k^2_\perp)/\xi^4}}. \tag{127}$$

In this case the delta functions imply a threshold value for k^2. The integral k^2 is handled in the fashion of Eq. (114c) by factoring out the square-root singularity and evaluating the rest of the integrand at the threshold value k^2_{th}. The remainder of the calculation follows the $q\bar{q}$ annihilation calculation; the final result for the quark–gluon scattering contribution to the parity-violating cross section is

$$\begin{aligned} d\sigma^{PV}_{\text{hadron}} \simeq{}& \frac{1}{8}\left(\frac{e_q}{e}\right)\left(\frac{e_l}{e}\right)\left(\frac{4}{3}\frac{\alpha_s}{2\pi}\right)\frac{\alpha}{Q^2 s}\frac{A_l V_q}{M_Z^2}\frac{d^3l^+\, d^3l^-}{l_0^+ l_0^-} \\ &\times e^{-|\mathbf{Q}_\perp|^2/\sigma^2}\left(\frac{|\mathbf{Q}_\perp|}{\sigma}\right)\left(\frac{|\boldsymbol{l}_\perp|}{\sigma}\right)(\hat{z}_\perp \cdot \hat{Q}_\perp x \hat{l}_\perp) \\ &\times q(x_1)\,\delta(x_1 - \bar{x}_1)\,dx_1\,G(x_2)\,dx_2\,\theta(x_2 - \bar{x}_2) \\ &\times \bar{x}_2^{5/2}(x_2 - \bar{x}_2)^{3/2}(x_2^2 + \bar{x}_2^2)^{-5/2}|(2x_2 - \bar{x}_2)/\bar{x}_2| \\ &\times e^{r_2}|(3 + 4r_2)\,I_0(r_2) + (1 + 4r_2)\,I_1(r_2)|. \end{aligned} \tag{128}$$

The numerical results for the asymmetry a^{PV} for the proton-proton collisions are plotted in Figs. 19. The numerator of the asymmetry is calculated by summing the quark–antiquark annihilation Eq. (118) and initial-gluon Eq. (128) contributions to the parity-violating cross section over quark flavor. The sum of all such asymmetry is calculated by summing the pure electromagnetic cross section Eq. (119) over quark flavor and dividing this sum by the squared u quark electric charge [cf. Eq. (53)]. The proton–proton asymmetry is expressed in the form

$$a^{PV}(pp) \equiv (\hat{z} \cdot \hat{Q}_\perp \times \hat{l}_\perp)\frac{A_l}{(e_l/e)}\frac{V_u}{(e_u/e)}\frac{\sigma|\boldsymbol{l}_\perp|}{M_Z^2}K(\tau, x_F, |\mathbf{Q}_\perp|/\sigma) \tag{129a}$$

$$\sim 3.5 \times 10^{-4}(\hat{z} \cdot \hat{Q}_\perp \times \hat{l}_\perp)\,K(\tau, x_F, |\mathbf{Q}_\perp|/\sigma) \tag{129b}$$

for the parameters of Eq. (120). The function $K(\tau, x_F, |\mathbf{Q}_\perp|/\sigma)$ is calculated using the proton parton distributions of Ref. [18] and gluon distribution of the form Eq. (55) with $n = 7$ (to match the $\bar{d}$ antiquark distribution). The result is plotted in Fig. 22.

The most striking feature of Fig. 22 is that the asymmetry arising from the quark-antiquark annihilation diagrams is roughly an order of magnitude less than the asymmetry arising from the initial gluon diagrams. This result can be understood by considering the structure of the annihilation and initial gluon contributions to the asymmetry.

For simplicity, assume that only one quark flavor contributes to the asymmetry. Then the initial gluon contribution to the parity-violating asymmetry involves the ratio of the gluon distribution (convoluted with the functional form shown in Eq. (128)) to the proton antiquark distribution, The initial gluon distribution used here is of the form Eq. (55) with $n = 7$, while, e.g., the $\bar{d}$ antiquark distribution is

$$\bar{d}(x) = 0.17 \frac{(1-x)^7}{x}. \tag{130}$$

By taking the ratio of these two distributions, it is seen that the initial gluon contribution to the asymmetry involves a large ratio $4/0.17 \sim 20$. The corresponding factor for the annihilation contribution—involving the ratio of a proton quark (or antiquark) distribution (convoluted with the functional form shown in Eq. (118)) to the same distribution—is of order unity. Therefore, the initial gluon contribution is larger than the annihilation contribution by an order of magnitude.

The parity-violating asymmetry in unpolarized proton-proton collisions is maximized for large (positive or negative) values of x_F but small ($\lesssim 0.10$) values of τ and for $|\mathbf{Q}_\perp| \sim 2\sigma \sim 1$ GeV. By symmetry, it vanishes at $x_F = 0$. Numerically the asymmetry is of the order of magnitude $A^{PV} \sim 0.01\%$ for $Q^2 \simeq 100\ \text{GeV}^2$ and typical parameter values.

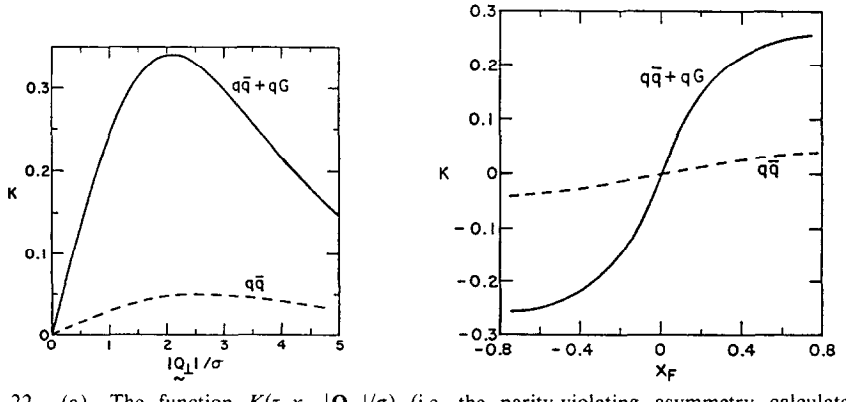

FIG. 22. (a) The function $K(\tau, x_F, |\mathbf{Q}_\perp|/\sigma)$ (i.e. the parity-violating asymmetry calculated for *unpolarized pp* collisions) is plotted versus $|\mathbf{Q}_\perp|/\sigma$. The other parameters are $\tau = 0.1$, $x_F = 0.5$. The solid line is a plot of the function with initial gluon and quark–antiquark annihilation contributions included. The broken line shows the annihilation contributions only. (b) The function $K(\tau, x_F, |\mathbf{Q}_\perp|/\sigma)$ is plotted versus x_F for $|\mathbf{Q}_\perp|/\sigma = 2$ and $\tau = 0.25$. The legend is the same as for (a).

V. Conclusions

It has been shown that the experimental study of weak asymmetries in lepton production from hadronic collisions could be very fruitful. The large dilepton masses which can be produced in such collisions (up to approximately 10 GeV in present experiments) may give rise to electromagnetic-weak interference effects of the order of a few percent of the total lepton pair production cross section. Effects of this size should be measurable.

Such electroweak interference effects give rise to several distinct types of asymmetries. These asymmetries consist of the ratio of a term in the differential electroweak cross section to the appropriate electromagnetic differential cross section. The electroweak interference contribution to the lepton pair production cross section from a polarized quark (and an unpolarized quark or gluon) in the context of the parton model augmented by perturbative QCD contains four distinct terms. Each term is distinguishable from the others by its symmetry under the parity operation and under the interchange of the final lepton pair momenta ("charge symmetry"). One of these four terms in the electroweak cross section conserves parity and is charge symmetric. This term is proportional to the electromagnetic cross section but is too small of a correction to be studied experimentally at present.

The remaining three terms give rise to three asymmetries, two of which violate parity and two of which are charge antisymmetric. For example, the term which gives rise to the "charge-helicity asymmetry" is charge-antisymmetric and violates parity, since it is also antisymmetric in the helicity of the polarized quark. Numerically, these asymmetries are of roughly the same order of magnitude. For a dilepton mass of 10 GeV, electroweak interference in the Weinberg–Salam model leads to a helicity asymmetry of order 0.1% and a charge-helicity asymmetry of order 1% in hadron–polarized hadron collisions. A charge asymmetry of the order of a few percent (not inclusing higher-order electromagnetic corrections [16]) is also predicted to occur in collisions of unpolarized hadrons.

The effects described above all occur within the framework of the parton model. Corrections to this simple picture occur through perturbative QCD. Within this framework the asymmetries were calculated in differential and integrated forms for comparison with experiment. The differential form consists of the ratio of electroweak to electromagnetic cross sections differential in the lepton pair momentum and evaluated at large transverse momentum. The leading contribution to both the numerator and denominator of this ratio is of order α_s; thus to the order calculated here this "differential" asymmetry is independent α_s.

An "integrated" asymmetry is defined to be the ratio of the electroweak to the electromagnetic cross section, each integrated over the transverse momentum of the lepton pair. The numerator and denominator of the integrated asymmetry both include terms of order $(\alpha_s)^0$ and higher.

The three integrated asymmetries were calculated previously in the context of the parton model [12–15]; here these same asymmetries are calculated to order α_s. Because each term in the electroweak cross section displays a different symmetry, it

might be expected that the corrections to each of them due to perturbative QCD are of different sizes numerically. In fact the order α_s corrections to the integrated charge-*antisymmetric* terms are approximately 10% larger than the corrections to the integrated charge-symmetric terms. Thus the integrated charge asymmetry and charge-helicity asymmetries (being the ratio of charge-antisymmetric to charge-symmetric integrated cross sections) are increased by perturbative QCD corrections in any kinematic region where quark–antiquark annihilation is the dominant mechanism for lepton pair production. This result was demonstrated explicitly for πp collisions.[4] On the other hand, corrections to the helicity asymmetry (which is the ratio of integrated charge-symmetric terms) are very small in valence quark processes like πp collisions despite large corrections to both the numerator and denominator of the asymmetry. Two questions of interest which were probed [13] earlier in the context of the parton model involved the parity-violating asymmetries predicted [12–15] to occur in lepton pair production from polarized hadrons. The first question arose from the consideration of π-polarized p collisions. In the parton model, the polarized u and d quark distributions in the proton can be determined [13] by measuring the parity-violating asymmetries in π^--polarized p and π^+-polarized p collisions, respectively. Of particular interest is the polarized d quark distribution. Calculations [26] based on perturbative QCD indicate that a quark carrying all the momentum of the parent proton should possess the same helicity as the proton. In combination with certain sum rules for the parton model weak asymmetries [13], this result indicates that the parity-violating asymmetries in $\pi^+ p$ collisions change sign as a function of the scaling variable—a rather dramatic experimental signature. This sign change also occurs in the $\pi^+ p$ parity-violating asymmetries calculated at large transverse momenta, as well as in the corresponding integrated asymmetries with perturbative QCD corrections included.

The second effect of interest in the parton model involved a probe of the flavor $SU(2)$ symmetry of the proton antiquark sea. If the $\bar{d}$ antiquark distribution falls off more slowly than the $\bar{u}$ antiquark distribution for large momentum fractions, a sign change can occur in the parity-violating terms in the proton–polarized proton cross section (and thus also in the corresponding asymmetries). If perturbative QCD corrections are included, however, the effect of initial gluon contributions to the cross section may serve to eliminate this sign change if the gluon distribution falls off more slowly than the antiquark distributions at large momentum fractions. For the proton antiquark sea of Ref. [18], and a gluon distribution of the form Eq. (55) with $n = 7$ or higher such a sign change does occur.

A parity violating effect may also occur in lepton pair production from collisions of *unpolarized* hadrons [19]. The existence of such an asymmetry requires specific assumptions about the nature of poles in the quark propagator, as well as the inclusion of nonperturbative aspects of confinement, and therefore goes beyond the

[4] Antiproton–proton collisions are not treated separately since the dominant pair production mechanism is presumably $u\bar{u}$ annihilation (see Ref. [13]) and therefore the weak asymmetries are numerically very similar to those calculated for $\pi^- p$ collisions.

usual treatment of perturbative QCD. However, should such an effect be observed experimentally it could provide a unique way of studying nonperturbative aspects of hadronic structure. With the use of several assumptions about the nonperturbative structure of hadrons a parity-violating effect of order 0.01% is predicted to occur for $Q^2 \simeq 100\ \text{GeV}^2$.

It has been shown that the measurement of various weak asymmetries can provide a new and unique way of observing the fundamental structure of hadrons. Perhaps in the near future the predictions made here will be tested experimentally.

At the conclusion of this work an analysis of similar questions appeared in the literature [36]. A calculation of the charge asymmetry in hadronic lepton pair production at Z^0 energies has also been published [37] by the present author.

ACKNOWLEDGMENTS

It is a pleasure to thank S. D. Ellis, E. M. Henley, P. Mockett, J. Rutherfoord, and R. W. Williams for many enlightening discussions. Conservations with S. Brodsky, S. D. Drell, F. Gilman, and T. Tsao were also very useful.

REFERENCES

1. J. CHRISTENSON *et al.*, *Phys. Rev. Lett.* **25** (1970) 1523; *Phys Rev. D* **8**, (1973), 2016.
2. S. D. DRELL AND T.-M. YAN, *Phys. Rev. Lett.* **25** (1970), 316; **25** (1970), 902; *Ann. Phys. (N.Y.)* **66**, (1971), 578.
3. R. P. FEYNMAN, "Photon–Hadron Interactions," Benjamin, Reading, Mass., 1973.
4. W. MARCIANO AND H. PAGELS, *Phys. Rep.* **36C** (1978), 137.
5. D. GROSS AND F. WILCZEK, *Phys. Rev. Lett.* **26** (1973) 1343; H. D. POLITZER, *Phys. Rev. Lett.* **26** (1973) 1346.
6. H. D. POLITZER, *Phys. Lett.* **70B** (1977), 430.
7. H. D. POLITZER, *Nucl. Phys. B* **129** (1977), 301; *Phys. Rep.* **14C**, (1972), 129.
8. R. K. ELLIS, M. MACHACEK, H. D. POLITZER, AND G. C. ROSS, *Phys. Lett.* **78B** (1978), 281; S. B. LIBBY AND G. C. STERMAN, *Phys. Lett.* **78B** (1978), 281.
9. C. T. SACHRAJDA, *Phys. Lett.* **73B**, (1978), 185; G. ALTARELLI, G. PARISI, AND R. PETRONZIO, *Phys. Lett.* **78B** (1978); 351; J. FRENKEL, M. J. SHAILER, AND J. C. TAYLOR, *Nucl. Phys. B* **148** (1979), 228; A. V. RADYUSHKIN, *Phys. Lett.* **69B** (1977), 245. See also A. J. BURAS, *Rev. Mod. Phys.* **52**, No. 1 (1980) and references therein; and Proceedings of the Summer Institute in Elementary Particle Physics, Boulder, Colorado, 1979.
10. G. ALTARELLI, R. K. ELLIS, AND G. MARTINELLI, *Nucl. Phys. B* **143** (1978), 52; **146** (1978), 544 Erratum; **157** (1979), 461; **160** (1979), 301.
11. F. HALZEN AND D. SCOTT, *Phys. Rev. D* **19** (1979), 216; J. KUBAR-ANDRE AND F. E. PAIGE, *Phys. Rev. D* **19** (1979), 221; K. HARADA, T. KANEKO, AND D. SAKAI, *Nucl. Phys. B.* **155** (1979), 169; **165** (1980), 545 Erratum; K. HARADA, *Phys. Rev. D* **22** (1980), 663; B. HUMPERT AND W. L. VAN NEERVEN, *Phys. Lett.* **84B** (1979), 327; **89B** (1979), 69.
12. D. J. E. CALLAWAY, *Phys. Rev. D* **23** (1981), 1547.
13. D. J. E. CALLAWAY, S. D. ELLIS, E. M. HENLEY, AND W.-Y. P. HWANG, *Nucl. Phys. B* **171** (1980), 59.
14. F. GILMAN AND T. TSAO, *Phys. Rev. D* **21** (1980), 159.
15. H. S. MANI AND S. D. RINDANI, *Phys. Lett.* **84B** (1979), 104.

16. R. W. Brown, V. K. Cung, K. O. Mikaelian, and E. A. Paschos, *Phys. Lett.* **43B** (1973); R. W. Brown, K. O. Mikaelian, and M. K. Gaillard, *Nucl. Phys. B* **75** (1974), 112; K. O. Mikaelian, *Phys. Lett.* **55B** (1975), 219; R. Budny, *Phys. Lett.* **45B** (1973), 340.
17. M. J. Alguard, *et al.*, *Phys. Rev. Lett.* **37** (1976), 1258; **37** (1976), 1261; **41** (1978), 70.
18. R. D. Field and R. P. Feynman, *Phys. Rev. D* **15** (1977), 2590.
19. D. J. E. Callaway, E. M. Henley, S. D. Ellis, and W.-Y. P. Hwang, *Phys. Lett.* **89B** (1979), 95.
20. S. Weinberg, *Phys. Rev. Lett.* **19** (1967), 1264; A. Salam, *in* "Elementary particle physics: relativistic groups and analyticity" (N. Svartholm, Ed.), p. 367, Almqvist and Wiksell, Stockholm, 1968.
21. S. L. Glashow, J. Iliopoulos, and G. Maiani, *Phys. Rev. D* **2** (1970), 1285.
22. J. D. Bjorken and S. D. Drell, "Relativistic Quantum Mechanics," McGraw–Hill, New York, 1964.
23. F. E. Close and D. Sivers, *Phys. Rev. Lett.* **39** (1977), 1116.
24. L. M. Sehgal, *Phys. Rev. D* **10** (1974), 1663.
25. Particle Data Group, *Rev. Mod. Phys.* **52** (1980), S1.
26. G. R. Farrar and D. R. Jackson, *Phys Rev. Lett.* **35** (1975), 1416; S. Brodsky, SLAC Summer Institute Lectures, 1979.
27. K. J. Anderson *et al.*, *Phys. Rev. Lett.* **42** (1979), 944.
28. H.-Y. Cheng and E. Fischbach, *Phys. Rev. D* **9** (1980), 860.
29. See, e.g., F. Halzen and D. M. Scott, *Phys. Rev. D* **21** (1980), 1320; V. Barger *et. al.*, *Phys. Lett.* **91B**, (1980), 253; **92B** (1980), 179; N. Fleishon and W. J. Stirling, *Nucl. Phys. B* **188** (1981), 205; and references contained therein.
30. G. 't. Hooft and M. Veltman, *Nucl. Phys. B* **44** (1972), 189; C. G. Bollini and J. J. Giambiagi, *Nuovo Cimento B* **12** (1972), 20.
31. W. J. Marciano, *Phys. Rev. D* **12** (1975), 3861.
32. G. Altarelli and G. Parisi, *Nucl. Phys. B* **126** (1977), 298.
33. G. T. Bodwin, C. Y. Lo, J. D. Stack, and J. D. Sullivan, *Phys. Lett.* **92B** (1980), 337; B. Humpert and W. L. van Neerven, *Phys. Lett.* **84B** (1979), 327; **85B** (1979), 471; Erratum: **85B** (1979), 293.
34. For a discussion of how such distribution functions may arise in leading logarithmic perturbation theory, G. Parisi and R. Petronzio, *Nucl. Phys. B* **154** (1979), 427; C. Y. Lo and J. D. Sullivan, *Phys. Lett.* **86B** (1979), 327; H. F. Jones and J. Wyndham, *Nucl. Phys. B* **176** (1980), 466; C. L. Basham, L. S. Brown, S. D. Ellis, and S. T. Love, *Phys. Lett.* **85B** (1979), 297; see also D. E. Soper, *Phys. Rev. Lett.* **43** (1979), 1847.
35. M. Abramowitz and I. A. Stegun, "Handbook of Mathematical Functions, Dover, New York, 1972.
36. P. Aurenche and J. Lindfors, *Nucl. Phys. B* **185** (1981), 274; **185** (1981), 301; M. Hayashi, S. Homma, and K. Katsuura, *J. Phys. Soc. Japan* **5** (1981), 1427.
37. D. J. E. Callaway, *Phys. Lett.* **108B** (1982), 421.